ORNL/TM-2024/3536

SCALE Analyses of Scenarios in the High-Temperature Gas-Cooled Reactor Fuel Cycle

Rabab Elzohery
Donny Hartanto
Friederike Bostelmann
William A. Wieselquist

October 2024

OAK RIDGE National Laboratory

ORNL IS MANAGED BY UT–BATTELLE, LLC, FOR THE U.S. DEPARTMENT OF ENERGY

ORNL/TM-2024/3536

Nuclear Energy and Fuel Cycle Division

SCALE ANALYSES OF SCENARIOS IN THE HIGH-TEMPERATURE GAS-COOLED REACTOR FUEL CYCLE

Rabab Elzohery
Donny Hartanto
Friederike Bostelmann
William A. Wieselquist

October 2024

Prepared by
OAK RIDGE NATIONAL LABORATORY
Oak Ridge, TN 37831-6283
managed by
UT-Battelle, LLC
for the
US DEPARTMENT OF ENERGY
under contract DE-AC05-00OR22725

CONTENTS

LIST OF FIGURES

LIST OF TABLES

ABBREVIATIONS

BUMS	burnup measurement and sorting system
CCR	criticality control rod
CCS	criticality control system
CE	continuous energy
CSAS	Criticality Safety Analysis Sequence
FHR	fluoride salt-cooled high-temperature reactor
FHSS	fuel handling and storage system
HALEU	high-assay low-enriched uranium
HPR	heat pipe reactor
HTGR	High-Temperature Gas-cooled Reactor
MG	multigroup
MSR	molten salt-fueled reactor
non-LWR	non-light water reactor
NRC	Nuclear Regulatory Commission
ORNL	Oak Ridge National Laboratory
PBR	pebble bed reactor
PF	packing fraction
PSP	protective structural packaging
SFR	sodium-cooled fast reactor
SFT	spent fuel tank
SNL	Sandia National Laboratories
TRISO	tristructural isotropic

ACKNOWLEDGMENTS

Support for this work was provided by the US Nuclear Regulatory Commission under IAA 31310022S0011.

ABSTRACT

This report demonstrates the SCALE code system's capabilities in modeling and simulating scenarios in the High-Temperature Gas-cooled Reactor (HTGR) nuclear fuel cycle as part of a United States Nuclear Regulatory Commission (NRC) project that aims to demonstrate the capabilities of the SCALE and MELCOR codes for non-light water reactor (non-LWR) modeling and simulation.

In the present study, four scenarios during four distinct stages of the HTGR fuel cycle were selected for demonstration using SCALE: UF_6 transportation, fresh fuel pebbles transportation, fuel utilization, and spent fuel storage. Analysis of these scenarios involved criticality calculations and the generation of fuel pebble inventory. For scenarios that required specifications of HTGR fuel pebbles or operating conditions, the characteristics of PBMR-400 was used. This was based on previous modeling and simulation work and because the specifications for the PMBR-400 are publicly available. It is important to note that some information in these scenarios, such as transportation package specifications and operational data, is based on publicly available information. Assumptions were made to fill in any missing information; these assumptions are stated where necessary.

The first scenario demonstrated SCALE criticality calculations during the UF_6 transportation stage, where the DN30-X transportation package containing UF_6 using high-assay low-enriched uranium (HALEU) was modeled. SCALE predicted that the package is subcritical under different conditions, including water ingress into the transportation package. The limiting case was that of the DN30-20 package with water between containers, where the k_{eff} value was found to be 0.64266 ± 0.00011.

The second scenario involved further SCALE criticality calculations but during the fresh fuel transportation stage (i.e., fresh TRISO pebbles). The Versa-Pac 55 transportation package was modeled using SCALE, and criticality calculations were performed using multigroup (MG) and continuous energy (CE) cross section libraries. For an infinite lattice of Versa-Pac packages containing fresh fuel pebbles, the spacing between packages was varied under dry conditions and different levels of water ingress. SCALE calculations showed that the package is significantly subcritical, with the most limiting conditions being when the package is flooded with water while the containers are touching, in which case k_{eff} was found to be 0.36714 ± 0.00011. The calculations demonstrated SCALE's capabilities for efficient MG calculations of double-heterogeneous fuel systems as well as recent enhancements for explicit tristructural isotropic fuel particle modeling in CE calculations.

Continuing along the fuel cycle, a third scenario during fuel utilization assumed a rupture in pipes that move the pebbles out of the core after each pass for inspection, causing the pebbles to exit the core. For this scenario, the SCALE capability for rapid inventory generation of fuel pebbles was demonstrated. The generated inventory was provided to the MELCOR team to study the accident progression, source term and consequences..

Finally, a scenario of damage to the spent fuel tank (SFT) storing discharged fuel was demonstrated. The SCALE capability for inventory generation and decay heat analysis was demonstrated by calculating the total fuel inventory of the tank, which was then shared with the MELCOR team for accident consequence analysis. The total decay heat of the SFT at the time it is full with discharged pebbles was computed and found to be 124 kW, with 3% of the decay heat being produced by less than 0.1% of the fuel pebbles.

The demonstration examples provided here show the readiness of the SCALE code for modeling and simulating scenarios within the HTGR fuel cycle; however, there remains potential for improvement of such analyses, as well as more realistic studies, that use economically optimized transportation packages and storage tanks, as more details about the HTGR fuel cycle are released to the public and as validation data become available.

1. INTRODUCTION

With the renewed global interest in non-light water reactor (non-LWR) designs and associated licensing demands, there has been a need to evaluate existing computer codes' capabilities to accurately model them. In response to this need, the Nuclear Regulatory Commission (NRC) has initiated a project to assess the modeling and simulation capabilities for accident progression, source term, and consequence analysis for non-LWR technologies. The two main codes included in this study are the SCALE code system (Wieselquist and Lefebvre 2023), developed and maintained by Oak Ridge National Laboratory (ORNL), and MELCOR (Humphries et al. 2021), developed and maintained by Sandia National Laboratories (SNL). The SCALE code is used for radionuclide inventory, decay heat, and shielding calculations, among other types of analysis, whereas MELCOR uses these data to perform accident consequence analysis.

The initial phase of this project aimed to calculate accident scenarios during operation. Five non-LWR designs were included in this project, for which SCALE models were developed. The designs are the pebble-bed High-Temperature Gas-cooled Reactor (HTGR) (Skutnik and Wieselquist 2021a), molten salt-fueled reactor (MSR) (Lo et al. 2022), the pebble-bed fluoride salt-cooled high-temperature reactor (FHR) (Bostelmann et al. 2022), the sodium-cooled fast reactor (SFR), (Shaw et al. 2023), and the heat pipe reactor (HPR) (Walker et al. 2021). More details about this work can be found in "Volume 3: Computer Code Development Plans for Severe Accident Progression, Source Term, and Consequence Analysis" (US NRC 2020).

The next phase of the project, described in "Volume 5: Radionuclide Characterization, Criticality, Shielding and Transport in the Nuclear Fuel Cycle" (US NRC 2021), aims to demonstrate the code's capabilities to simulate scenarios during various stages of the non-LWR fuel cycle. To meet this goal, representative nuclear fuel cycles for the aforementioned five non-LWRs designs were developed based on publicly available information, and potential hazards and accident scenarios in each fuel cycle stage were identified (Bostelmann et al. 2023). A number of these identified scenarios for each design were selected to demonstrate the SCALE and MELCOR codes' modeling and simulation capabilities concerning the fuel cycle.

The present study focused on one of these designs, the HTGR, the main goal of which is to demonstrate SCALE capabilities for simulating scenarios in the HTGR fuel cycle. The stages of the HTGR fuel cycle are elaborated on in a previous report in Bostelmann et al. (2023), but for the sake of completeness, the basic stages are outlined in Figure 1.

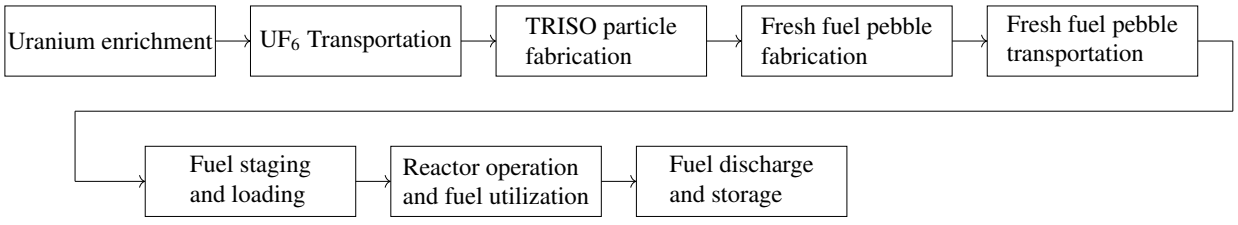

Figure 1. HTGR fuel cycle stages.

In this study, four stages were selected for demonstration, and specific accident scenarios were simulated within each stage. These stages and the specific scenarios are summarized as follows:

1. UF_6 transportation
    - **Scenario 1**: Water ingress into an infinite lattice of transportation containers at optimal moderator-to-fuel ratio, potentially leading to a criticality accident.

2. Fresh fuel pebble transportation
    - **Scenario 2**: Damage/drop of a transportation container leading to reduced container spacing and a potential criticality accident.
3. Reactor operation and fuel utilization
    - **Scenario 3**: fuel handling and storage system (FHSS) pipe rupture leading to pebbles exiting the reactor with high temperature and pressure, potentially leading to graphite and air interaction as well as fission product and graphite dust release.
4. Onsite storage of spent fuel
    - **Scenario 4**: Collision of vehicle or suspended load with storage tank causing damage to tank and damage to pebbles inside the tank, causing fission product and graphite dust release.

SCALE analysis of these scenarios included criticality calculations for scenarios 1 and 2, fuel inventory, and decay heat calculations for scenarios 3 and 4. The calculated fuel inventory was shared with MELCOR team for accident progression analysis (US NRC, ORNL, SNL 2023).

The PBMR-400 (Reitsma et al. 2013) was used as a reference reactor throughout this study. It is a 400 MWth pebble-bed HTGR cooled by helium and was originally considered for development by the South African utility ESKOM as part of a larger industrial consortium, PBMR Ltd., which also included the South African Government and British Nuclear Fuel.

Figure 2 shows a SCALE PBMR-400 model for the initial phase of this project (Skutnik and Wieselquist 2021b). Information used in the model is based on data provided in the benchmark specification (Reitsma et al. 2013).

The PBMR-400 fuel pebble is 6 cm in diameter, and these spherical pebbles contain tristructural isotropic (TRISO) particles dispersed within a graphite matrix and surrounded by an outer fuel-free graphite zone. The full reactor core consists of approximately 452,000 fuel pebbles.

SCALE models of the fuel pebble and the TRISO particle are shown in Figures 3a and 3b, respectively. Table 1 shows the main characteristics of the fuel.

Table 1. PBMR-400 key characteristics

Characteristics	Value (Reitsma et al. 2013)
Fuel	UO_2
Fuel enrichment	9.6 wt.% ^{235}U
TRISO packing fraction within a pebble	9%
Number of TRISO particles in a pebble	15,000
Uranium content per pebble	9 g
Diameter of pebble	6 cm

The rest of the report is organized as follows: SCALE tools and analysis approaches are described in section 2. Description and analysis of the four selected HTGR scenarios are presented in Sections 3, 4, 5, and 6. Conclusions from this study are given in Section 7.

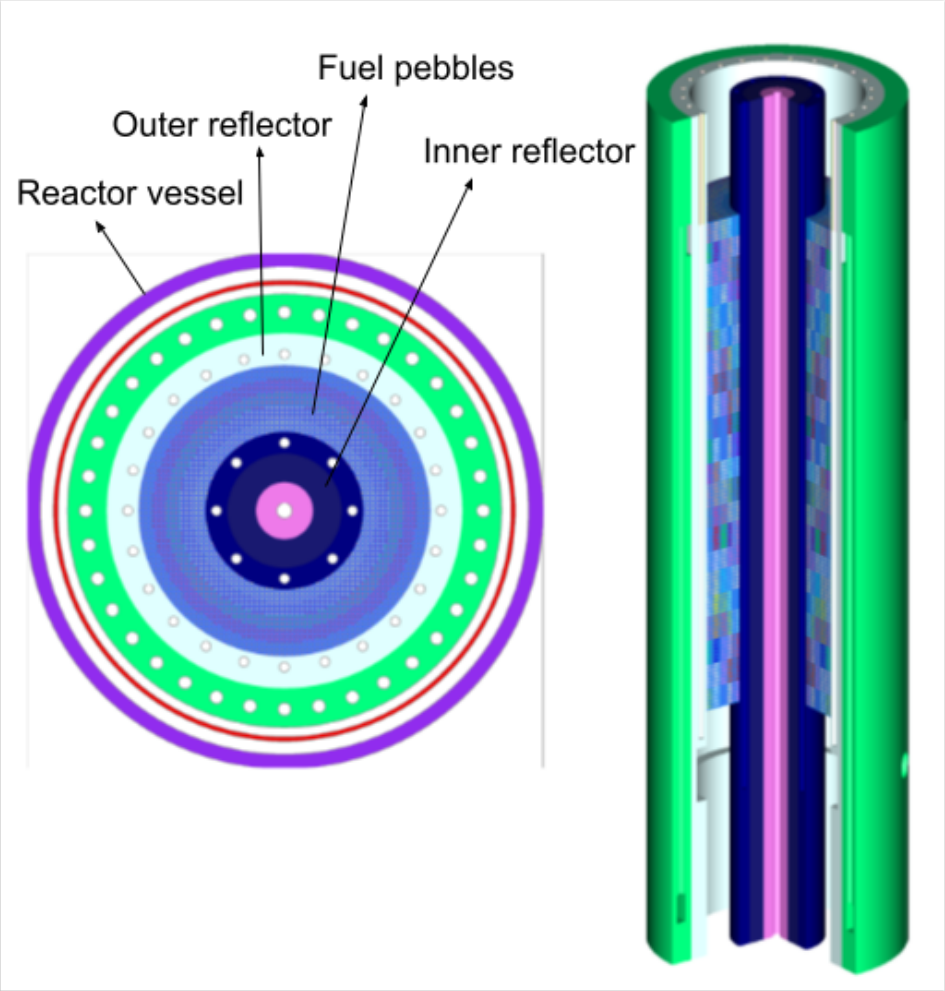

Figure 2. SCALE model of the PBMR-400 (left: XY view through the axial center; right: 3D view) (Skutnik and Wieselquist 2021b).

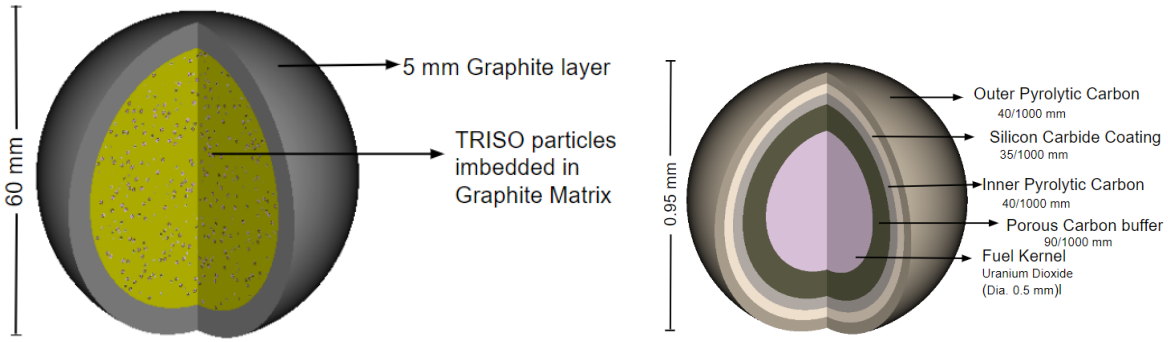

(a) PBMR-400 fuel pebble **(b) PBMR-400 TRISO particle**

Figure 3. SCALE models of the PBMR-400 fuel pebble and TRISO particle.

2. SCALE TOOLS AND ANALYSIS APPROACHES

SCALE is a comprehensive modeling and simulation suite for nuclear safety analysis and design developed by ORNL (Wieselquist and Lefebvre 2023). SCALE includes various capabilities such as criticality calculations, shielding, and inventory and decay heat computations. Moreover, SCALE 6.3 and SCALE 7.0 beta come with MG and pointwise CE nuclear data libraries processed from ENDF/B-VII.1 (Chadwick et al. 2011) or ENDF/B-VIII.0 (Brown et al. 2018) evaluated nuclear data files.

In the present study, the two library versions were used in different scenarios, as will be shown, and two main types of analysis were performed using development versions of SCALE 7.0. These analyses are briefly described below.

1. **Criticality calculations**: These calculations were performed for scenarios 1 and 2, for which the Criticality Safety Analysis Sequence (CSAS) within SCALE was employed. CSAS automates the cross section processing and the execution of Monte Carlo neutron transport calculations. This sequence encompasses two Monte Carlo codes: KENO and Shift. KENO (Goluoglu et al. 2011) has two variants, employing the exact transport solver but with different geometry packages. These variants are KENO-VA and KENO-VI, denoted as *CSAS5* and *CSAS6*, respectively. On the other hand, Shift (T. M. Pandya et al. 2016), a recently developed Monte Carlo tool was designed to provide particle transport capabilities on both KENO-VA and KENO-VI geometries, for which the sequences are denoted by CSAS5-Shift and CSAS6-Shift, respectively. More importantly, Shift is highly optimized, featuring advanced parallelization schemes that enable it to scale effectively across various systems. The present study used the SCALE sequence CSAS6-Shift.

2. **Inventory and decay heat calculations**: These calculations were performed for scenarios 3 and 4 using different SCALE sequences, codes, and utility modules, as described below.

    - **ORIGEN**: the depletion and decay solver code for time-dependent isotopic inventory and activities of materials (Gauld et al. 2011). ORIGEN can be used as a standalone code and also within various SCALE sequences. In this analysis, ORIGEN as a standalone code was specifically used to decay the isotopic inventory to some period after the specified accident.

    - **TRITON**: this sequence computes time-dependent composition and automates cross section processing, transport calculation to generate flux needed to compute one group cross sections, and finally passes these cross sections to ORIGEN to step initial material composition forward in time (De Hart and Bowman 2011). TRITON can use different transport solvers within SCALE, such as XSDRN for 1D problems, NEWT for 2D problems, and KENO and Shift for 3D problems. In this study, TRITON was used to generate ORIGEN reactor libraries for the PBMR-400 reactor at different burnup points and radial channels in the core. KENO was used within TRITON to perform the transport calculations.

    - **ORIGAMI**: this code rapidly computes the inventory of individual pebbles by automating the interpolation of pre-generated ORIGEN reactor libraries based on the user input. To accommodate flowing fuel such as that of pebble bed reactors (PBRs), ORIGAMI was extended to allow the user to define a history of individual pebbles that takes into account the change in power it experiences as it moves through the core, in addition to the time it spends in each axial region within different passes (Skutnik, Bostelmann, and Wieselquist 2022). In this analysis, ORIGAMI was used to compute the inventory of individual PBMR-400 pebbles using the cross sections pre-generated with TRITON and specification of the reactor, such as the number of passes, power profile, and temperature.

- **OBIWAN**: this command-line utility tool is used in SCALE for various post-processing purposes. In the analysis presented herein, OBIWAN was used for:
  - Blending the fuel inventory of the number of individual pebbles to compute an average pebble inventory
  - converting the binary concentration file (**f71**) to an inventory interface `ii.json` file for convenient data processing.

3. SCENARIO 1: WATER INGRESS INTO PACKAGES DURING UF_6 TRANSPORTATION

The HTGR fuel cycle stage addressed in this section is the transportation of the UF_6. The selected scenario involves assessing the package criticality under water ingress; thus, SCALE was used to perform criticality calculations.

The following section describes the transportation package used in this study, followed by an overview of the SCALE model and criticality results under nominal and accident conditions.

3.1 DN30-X PACKAGE DESCRIPTION

The DN30-X transportation package, developed by Orano (Orano 2022; US NRC 2023), was selected for this study. The package is similar to the DN30 transportation package (DAHER 2019; US NRC 2019) that has been used for uranium hexafluoride (UF_6) transportation up to an ^{235}U enrichment of 5% wt for years. In contrast to the DN30 package, the DN-30X package was only recently certified to transport UF_6 with ^{235}U enrichment up to 20 wt%. The"X" in DN30-X refers to the two design options for the package: DN30-10 and DN30-20. The 10 and 20 refer to the maximum allowable enrichment for each specific design. The DN30-10 is certified for transportation of UF_6 with ^{235}U enrichments up to 10 wt%, whereas the DN30-20 is certified for transportation of UF_6 with ^{235}U enrichment up to 20 wt%.

The package consists of two main components:

1. 30B-X cylinder
2. protective structural packaging (PSP)

The 30B-X cylinder is shown in Figure 4 and consists of a steel shell with an elliptical head on each end. The 30B-X cylinder is identical to the standard 30B cylinder, approved for transporting UF_6 with a maximum enrichment of 5% and used in the DN30 package. However, the 30B-X contains an interior criticality control system (CCS). This CCS consists of several criticality control rods (CCRs) made of steel rods filled with boron carbide (B_4C), in addition to three lattice holders that provide structural support for the control rods. The main distinction between the 30B-10 and the 30B-20 cylinders is the number of control rods: the former contains 33 control rods, and the latter contains 43 control rods. The permissible masses of UF_6 are 1460 and 1271 kg for the 30B-10 and 30B-20 cylinders, respectively.

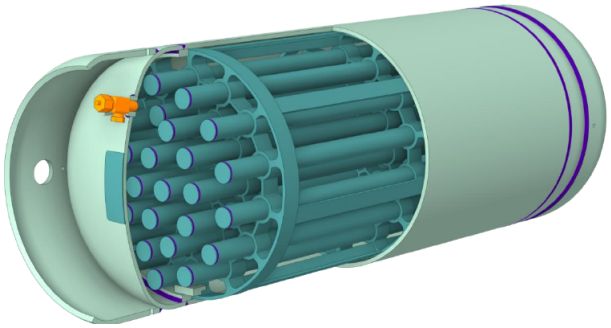

Figure 4. 30B-X cylinder (Orano 2022). Courtesy of Orano.

The PSP shown in Figure 5 provides thermal and structural protection for the inside cylinder during transportation, and it shares the same design used to transport standard 30B cylinders. It consists of two steel

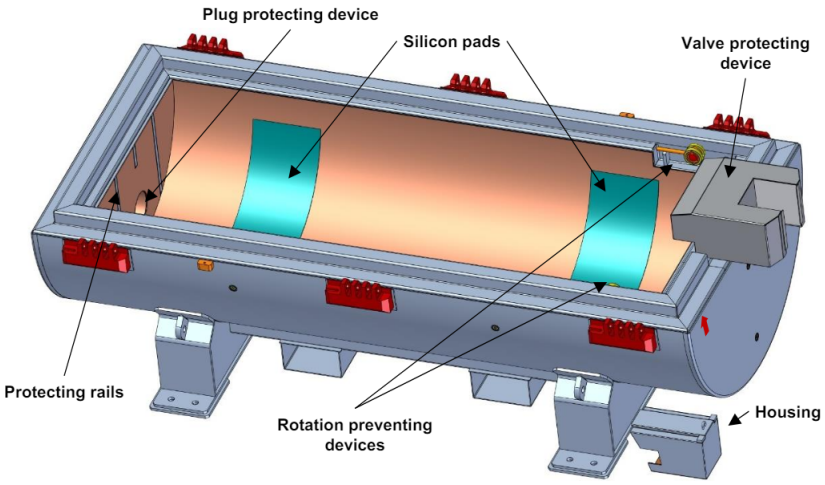

Figure 5. PSP overview (Orano 2022). Courtesy of Orano.

shells with layers of foam and other microporous material in the cavity between these shells that provide thermal insulation. Additional components of the PSP include a valve, plug, and silicon pads.

A more comprehensive description of the package can be found in the publicly available safety analysis report (Orano 2022).

3.2 SCALE MODEL OF THE DN30-X

SCALE 3D models of the two package variations (i.e., DN30-10 and DN30-20) were developed for CSAS-Shift calculations using dimensions and material specifications given in the safety analysis report.

Figure 6a shows a 3D cut of the SCALE model of the 30B-10 cylinder with its two elliptical heads and the long skirts, whereas Figure 6b shows a SCALE model of the cylinder with the enclosing PSP. Figures 7a and 7b show XY views of 30B-10 and 30B-20 cylinders, respectively.

Reflective boundary conditions are applied to represent an infinite hexagonal lattice of packages with the packages touching each other. As mentioned in Section 2, the SCALE sequence CSAS6-Shift was used to perform criticality calculations.

The following modeling assumptions and simplifications were applied:

1. Lattice holder, valve, plug, and nameplate are neglected.
2. The foam material in the PSP is neglected.
3. UF_6 is assumed at a theoretical density of 5.5 g/cm^3 with 0.5 wt% HF impurities.
4. Cylinders are 100% filled with UF_6, which exceeds the permissible mass for the 30B-10 and 30B-20 cylinder: this increase in UF_6 mass was 137% for the 30B-10 cylinder and 150% for the 30B-20 cylinder.
5. Cylinder 30B-10 was filled with UF_6 at the enrichment of the PBMR-400, which is 9.6% wt, whereas the 30B-20 cylinder was filled with UF_6 at the maximum allowed enrichment for this specific design, 20%.

Note that these assumptions are similar to those adopted in the safety analysis report (Orano 2022) and are conservative from a criticality safety perspective:

- The UF_6 density of 5.5 g/cm^3 is derived from a linear extrapolation of tabulated UF_6 density values to -40°C and which is larger than the density of 5.1 g/cm^3 at room temperature by a large margin and therefore conservative.
- The lattice holder and nameplate are made of stainless steel which contribute to parasitic absorption. Neglecting these modeling details and therefore neglecting the slight reactivity reduction is a conservative modeling choice.
- Filling the cylinder beyond the permissible mass limits results in additional fuel contained in the model and therefore conservative conditions.

Other components such as valve and plug (made of aluminum bronze alloy) and foam (made of polyisocyanurate, a low density materiel), are not expected to have a significant neutronic impact and have therefore been neglected for model simplification.

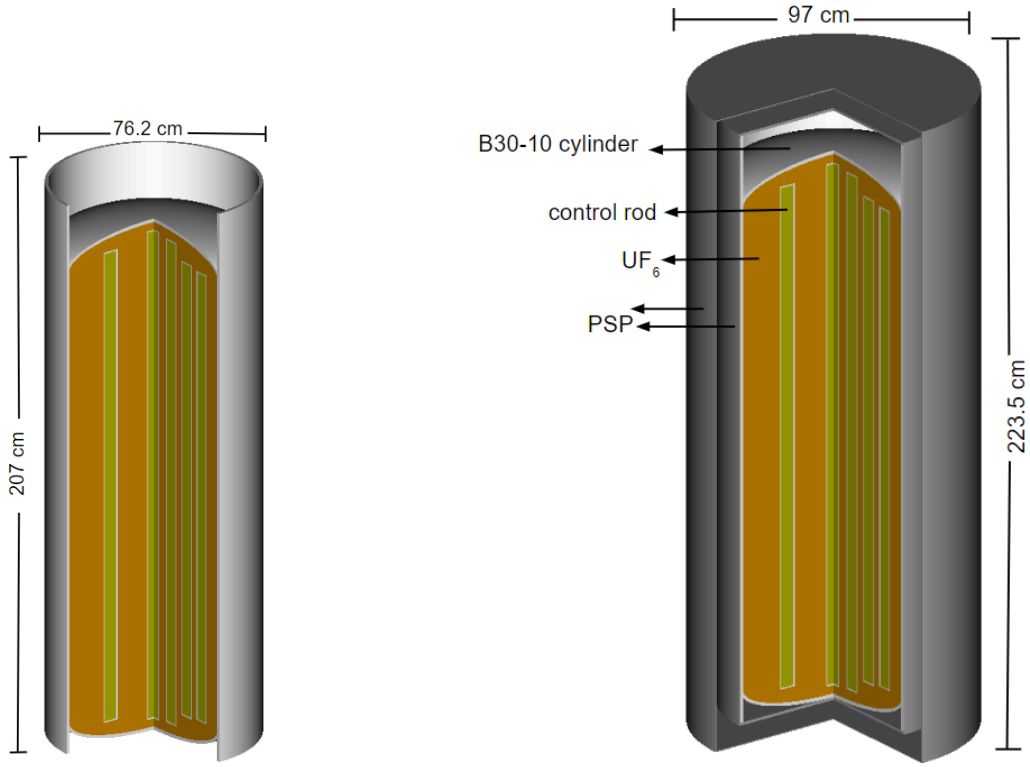

(a) SCALE model of the 30B-10 package **(b) SCALE model of the DN30-10 cylinder**

Figure 6. 3D view of the DN30-X SCALE model.

3.2.1 Baseline Model Results

The baseline model represents an infinite lattice of transportation packages where the packages are touching each other and are surrounded by air at room temperature. The DN30-10 and DN30-20 models were run with the SCALE CSAS-Shift sequence in CE mode using the ENDF/B-VII.1 (Chadwick et al. 2011) and ENDF/B-VIII.0 (Brown et al. 2018) cross section libraries, respectively. The calculations were run until a k_{eff} convergence of about 10 pcm was achieved. Table 2 shows the resulting k_{eff} for both package variations and the different cross section libraries.

Notable in these results is the very good agreement between calculations with the two cross section libraries: only 90 ± 15 pcm and 11 ± 16 difference for the DN30-10 and the DN30-20 package, respectively. Note that

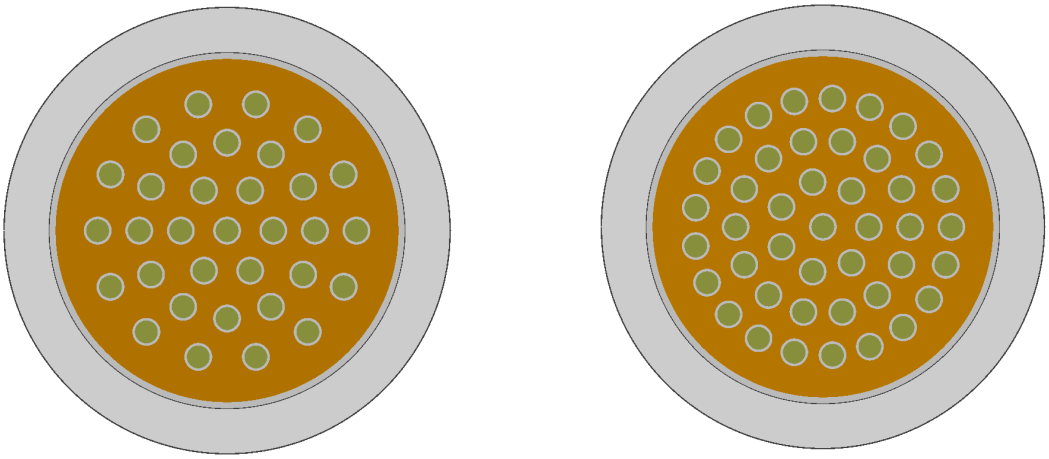

(a) DN30-10 (33 control rods) **(b) DN30-20 (43 control rods)**

Figure 7. XY view of the DN30-X SCALE model.

Table 2. DN30-X SCALE model k_{eff} results

Cross section library	DN30-10	DN30-20
ENDF/B-VII.1 CE	0.58459 ± 0.00011	0.77772 ± 0.00011
ENDF/B-VIII.0 CE	0.58549 ± 0.00010	0.77761 ± 0.00011

under nominal conditions, an infinite lattice of either package has a large margin for criticality, where k_{eff} is below the standard safety limit of 0.95, even though the packages are filled with UF_6 masses that exceed the maximum allowable masses.

3.3 ACCIDENT SCENARIOS DEMONSTRATION

The accident scenario selected for study here is water ingress into the package. Two variations of the scenario were simulated, as described below.

3.3.1 Scenario 1A: Water between Containers

In this scenario, water was introduced between containers, that is, in the volume surrounding the PSP—meaning that no water entered the package interior. This scenario is illustrated in Figure 8.

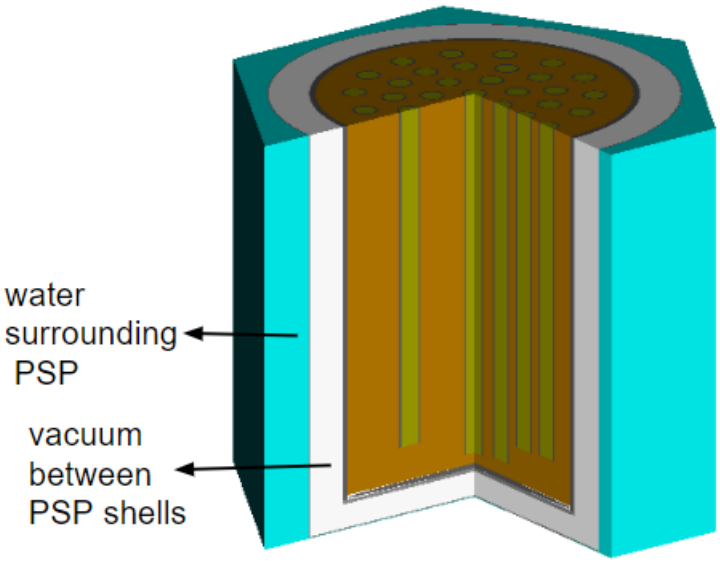

Figure 8. DN30-20 package SCALE model with water between containers (cut through midline).

Models of an infinite array of packages were generated by increasing the distance (i.e., edge-to-edge spacing) between the packages, ranging from 0 to 30 cm, and the water volume between packages accordingly. Similar to the baseline model, CSAS-Shift was used to run the calculations. However, only the ENDF/B-VII.1 cross section library was used in this case because there was no significant difference in baseline model results between the two cross section libraries. The calculated k_{eff} values are shown in Figures 9a and 9b, respectively.

The same trend was observed in both packages: k_{eff} decreases with increasing the pitch between packages, and the most limiting case was that in which the packages touch each other. In this case, k_{eff} was 0.51033 ± 0.00011 for the DN30-10 package and 0.64266 ± 0.00011 for the DN30-20 package. Increasing the distance and the water volume between containers increases the likelihood of neutron absorption in water before reaching the neighboring containers, reducing the system k_{eff}. Note that this also caused the k_{eff} for the touching containers to decrease compared to the baseline model results with air instead of water surrounding the packages.

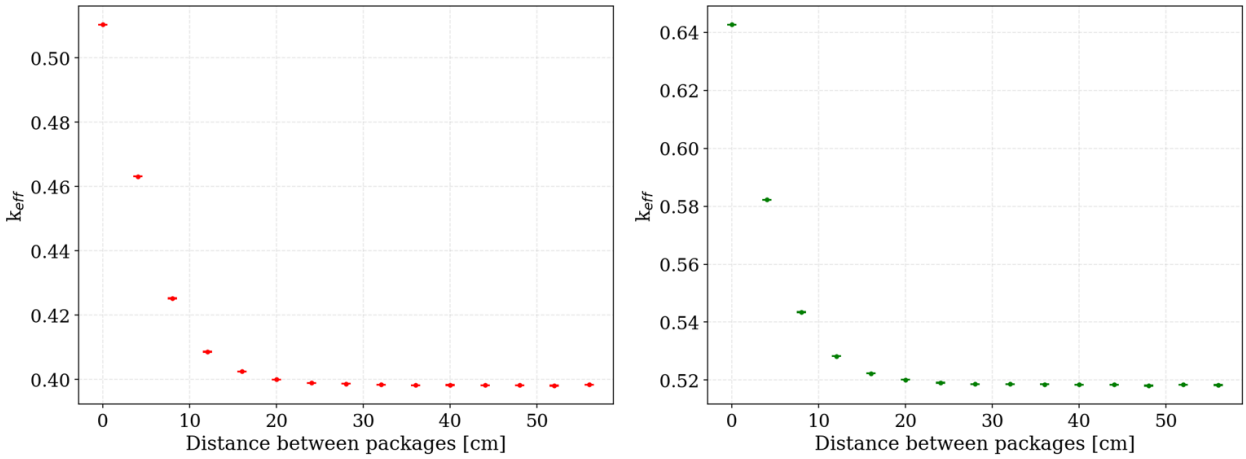

(a) DN30-10 **(b) DN30-20**

Figure 9. k_{eff} results as a function of container distance for an infinite lattice of DN30-X packages with water between the packages. Error bars represent 1σ statistical uncertainties from the Monte Carlo calculation).

Overall, all considered configurations with water between containers were found to be subcritical with a large margin to criticality; therefore, there is no criticality accident hazard under such conditions.

3.3.2 Scenario 1B: Water Ingress into the PSP

In this scenario, the water volume has been extended to the interior of the PSP, but not inside the 30B-X cylinder, as illustrated in Figure 10 for the DN30-20 package. This means that the system now includes water both outside the PSP and in the cavity between the two steel shells of the PSP.

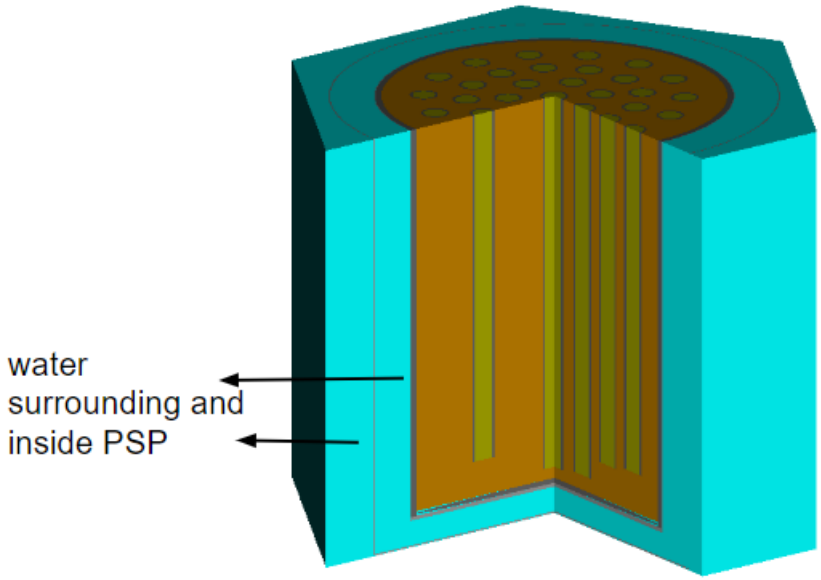

Figure 10. SCALE model of the DN30-20 package with water ingress between containers and inside the PSP (cut through the midline).

Like the previous scenario, the packages edge-to-edge spacing was increased incrementally from 0 to 30 cm.

The k_{eff} values are shown in Figures 11a and 11b respectively. As the figures show, the behavior here was found to be consistent with that of the previous scenario: k_{eff} decreases as the distance between containers increases. From a distance of ~20 cm on, k_{eff} remains constant within statistical uncertainty. However, k_{eff} exhibits generally lower value due to increased absorption rate in the increased water volume, with the most limiting case being when the packages touch each other, where k_{eff} is 0.43482 ± 0.00011 for the DN30-10 package and 0.54919 ± 0.00011 for the DN30-20 package.

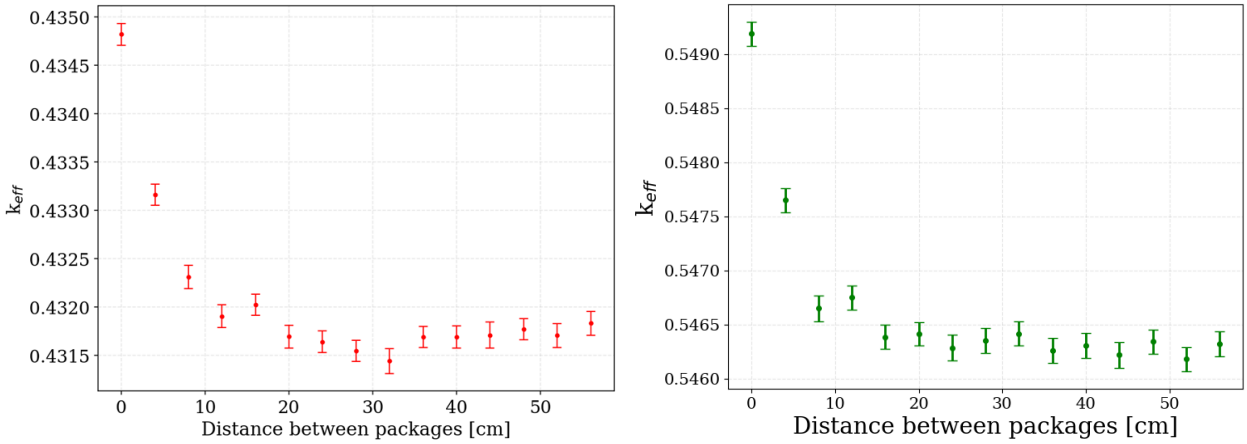

(a) DN30-10 **(b) DN30-20**

Figure 11. k_{eff} of DN30-X package with water ingress between containers and inside the PSP. Error bars represent 1σ statistical uncertainties from the Monte Carlo calculation.

Again, the system was found to be significantly subcritical, and no criticality accident hazard is anticipated under such conditions.

4. SCENARIO 2: DAMAGE/DROP DURING FRESH FUEL PEBBLE TRANSPORTATION

This section demonstrates the use of the SCALE code to simulate accident scenarios during the fresh fuel transportation stage of the HTGR fuel cycle. The scenario of interest is damage to or drop of transporting containers, leading to a change in spacing between them. The SCALE analysis includes criticality calculations during nominal and accident conditions.

The following section describes the transportation package used in this study, followed by the SCALE model overview and the results of nominal and accidental conditions.

4.1 VERSA-PAC 55 PACKAGE DESCRIPTION

The Versa-Pac package, developed by Orano, was selected for this study because it is a package approved by the NRC for transporting fresh fuel pebbles. The package specifications are taken from a safety analysis report published by the NRC (DAHER-TLI 2018; US NRC 2022). An illustration of the package is shown in Figure 12.

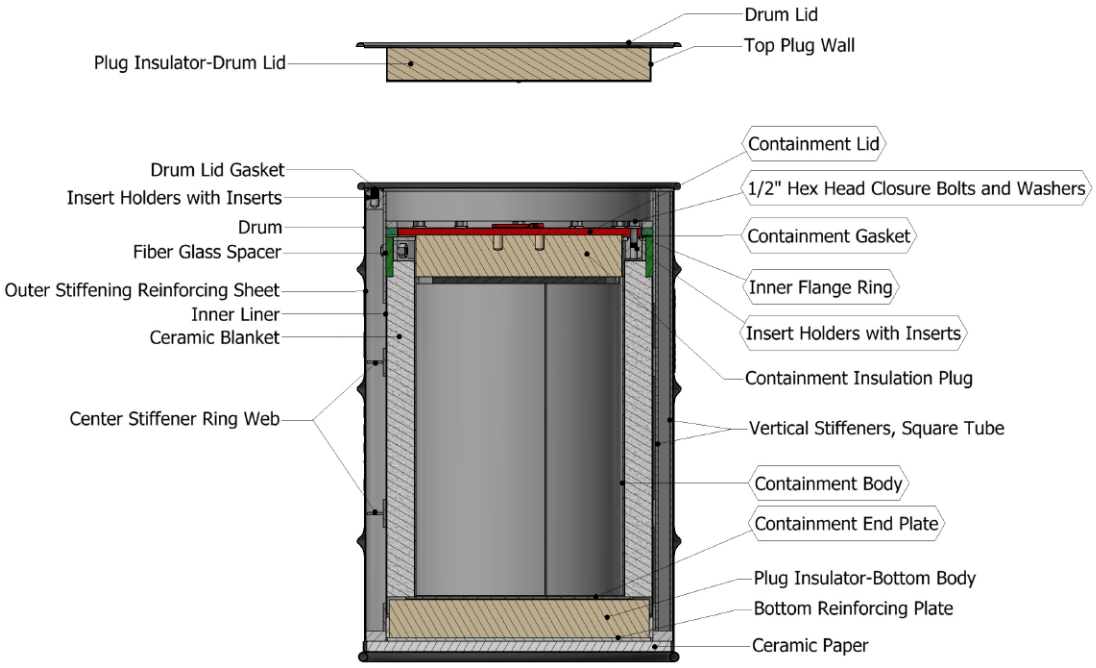

Figure 12. Versa-pack package (DAHER-TLI 2018). Courtesy of Orano.

The package consists of an inner payload vessel, where the fuel pebbles are loaded. The vessel is positioned inside a 55 gallon drum; thus, it is known as *VP-55*, which is used to refer to the package for the rest of this section. Another variation of the package has a 110-gallon drum known as VP-110, but it is not considered in this study because it was found that given the maximum permissible mass of ^{235}U for enrichment ranges of the PBMR-400 fuel enrichment, the container cannot be fully loaded with pebbles. The inner containment is completely insulated with appropriate ceramic fiber blankets and polyurethane foam layers. The VP-55 standard configuration shipping packages are designed to transport Type *A* fissile materials limited to ^{235}U masses based on the loading limits. For enrichments between 5 and 10 wt% ^{235}U, such as that of the PBMR-400 fuel, the maximum mass limit of ^{235}U is 505 g.

4.2 SCALE MODEL OF THE VERSA-PAC 55

A computational model of the VP-55 package was developed using SCALE. CSAS6-Shift, as described in Section 2, was used to perform the criticality calculations.

Two distinct models were developed, one employing a CE approach and the other a MG approach.

In the CE model, the TRISO fuel particles are explicitly modeled and randomly distributed within the graphite matrix. For the placement of TRISO particles at random locations, Shift's latest enhancement for automatic random placement was used. This feature is highly user-friendly, requiring only the definition of the TRISO particle packing fraction, after which the particles are randomly placed within the designated volume. See T. Pandya et al. (2023) and Ghaddar et al. (2024) for the latest enhancements in Shift with respect to this modeling feature.

The MG model utilizes SCALE's **double-het** approach, which prepares accurate self-shielded cross sections for the fuel zone. Note that the self-shielding calculation for such fuel is particularly challenging because of the different levels of heterogeneity resulting from the TRISO particles' dispersion in the graphite medium and the fuel pebbles' packing in a specified system. For details about the employed self-shielding methodology, the reader may refer to Kim et al. (2021) and Bostelmann et al. (2020).

In both the CE and the MG model, the fuel pebbles are randomly distributed inside the payload vessel. Table 3 shows the number of pebbles at different packing fractions inside the container and the associated mass of the ^{235}U. Note that the mass of ^{235}U does not exceed the maximum allowed limit for the PBMR-400 fuel enrichment, 9.6 wt%.

Table 3. Different pebble packing fractions and the associated ^{235}U mass at enrichment of 9.6 wt.% in the SCALE VP-55 model

Packing fraction (%)	Number of pebbles	^{235}U mass content (grams)
45	298	258
50	331	286
55	364	315
60	397	343

Details regarding the insulation and thermal materials are not adequately specified in publicly available documents, as they vary based on the fabrication process and possibly the manufacturers. However, the safety analysis report (DAHER-TLI 2018) provides density ranges for these materials. These materials are fiberglass, ceramic blanket, and polyurethane; the isotopic compositions for these materials are based on information provided in the compendium of material composition data for radiation transport modeling (Detwiler et al. 2021). The materials utilized in this model have been verified to fall within the specified range. For carbon steel materials, SCALE's standard composition was used. Reflective boundary conditions were employed to simulate an infinite lattice of packages.

Figure 13 shows a 3D visualization of the SCALE model.

4.2.1 Baseline Model Results

A baseline model was used to obtain reference results under nominal conditions and to understand the impact of different cross section libraries on k_{eff}. This model consists of an infinite lattice of VP-55 packages filled with fresh fuel pebbles at a packing fraction of 55%. The packages were assumed to be surrounded by air at room temperature. The packages were modeled in the tightest possible configuration: in a hexagonal lattice with containers touching, meaning the hexagonal lattice pitch equals the package diameter.

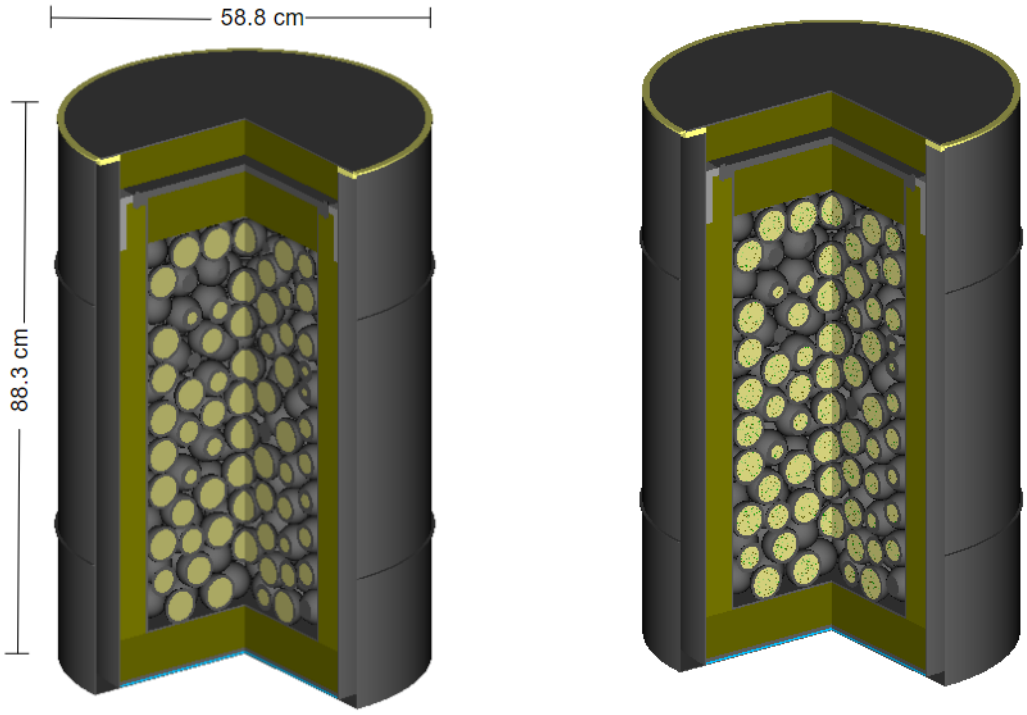

(a) MG model **(b) CE model (TRISO particles are modeled explicitly)**

Figure 13. 3D SCALE model of the VP-55 with packing fraction of 55%.

CE and MG calculations of this baseline model were performed using the CE and the 252-group cross section libraries, respectively, based on the ENDF/B-VII.1 (Chadwick et al. 2011) and (Brown et al. 2018) ENDF/B-VIII.0 nuclear data libraries. All models were run until a statistical uncertainty of approximately 10 pcm was attained.

Shown in Table 4 are the baseline results, which show an excellent agreement between the CE model and the MG models. This result confirms the adequacy of the MG cross section generation and the excellent performance of SCALE's MG doublehet implementation. Notably, good agreement was also observed between the two library versions—ENDF/B-VII.1 and ENDF/B-VIII.0—with a difference of 188 ± 14 pcm for the CE library and 193 ± 14 pcm for the MG library, the k_{eff} of the ENDF/B-VIII.0 version being consistently higher. This is consistent with previous analyses of graphite-moderated TRISO-fueled systems and can be explained by updates in the ^{235}U and ^{238}U cross sections in ENDF/B-VIII.0 compared to ENDF/B-VII.1 (Bostelmann et al. 2020). Regarding run time, the MG model exhibited a speedup of about four times compared to the CE run time.

Table 4. VP-55 SCALE model k_{eff} results

Cross section library	$k_{eff} \pm \sigma$	Δk_{CE-MG} (pcm)
ENDF/B-VII.1 CE	0.30387 ± 0.00010	ref
ENDF/B-VII.1 252g	0.30292 ± 0.00010	29 +/- 14
ENDF/B-VIII.0 CE	0.30575 ± 0.00010	ref
ENDF/B-VIII.0 252g	0.30486 ± 0.00010	90 +/- 14

To rule out a bias of results by the chosen random distribution of pebbles in the container, ten realizations

of the pebbles' coordinates in the container were generated, and calculations with these realizations were repeated. For these ten cases, the ENDF/B-VII.1 MG model was run, and the average k_{eff} was 0.30406 ± 0.00003. The difference between this average and the MG result reported in Table 4 is 10 ± 10 pcm, implying that the impact of the chosen random distribution of pebbles is negligible.

4.3 ACCIDENT SCENARIO DEMONSTRATION

In this section, two variations of an accident are demonstrated: (1) damage to or drop of containers under dry conditions and (2) damage to or drop of containers with simultaneous water ingress into the container.

4.3.1 Scenario 2A: Impact of Damage/Drop on Criticality for VP-55

It was assumed that damage to or drop of the containers would change the spacing between them, which can be simulated with SCALE by incrementally varying the distance between packages. Therefore, in the model of an infinite hexagonal lattice, the lattice pitch was varied, resulting in a perturbation of the packages edge-to-edge spacing from 0 to 30 cm. Calculations were performed for pebble packing fractions (PFs) of 45%, 50%, 55%, and 60% with the ENDF/B-VII.1 252-group library.

The k_{eff} values are shown in Figure 14. The figure shows an interesting behavior: the value of k_{eff} increases with increasing distance between containers until approximately 20 cm, after which it almost levels off. Although the maximum increase is only about 290 ± 11 pcm, this behavior suggests that the system is under-moderated, and as the distance between packages increases, the neutrons are allowed to thermalize between containers, increasing the fission rate and, accordingly, k_{eff}.

Overall, the predicted k_{eff} values in all cases are significantly subcritical and far below the safety limit of 0.95; thus, a criticality accident under such conditions is not anticipated.

4.3.2 Scenario 2B: Impact of Water Ingress into the Package

This scenario is similar to the previous one; however, water was introduced into the system, and two cases were studied. The first case involves water between packages, and the second is a more extreme scenario in which water is introduced into the package.

In both cases, the lattice pitch was varied, resulting in a perturbation of the packages edge-to-edge spacing from 0 to 30 cm. These calculations were performed for a pebble PF of 55%. Figure 15 shows the resulting k_{eff} in both cases.

In contrast to the dry case in Section 4.3.1, k_{eff} decreases with increasing distance between containers. The behavior is expected because as the distance between containers increases, the likelihood of neutron absorption in water increases before reaching the neighboring container, thereby worsening the thermal utilization factor, and thus k_{eff} decreases. It can also be observed the k_{eff} is significantly higher in the case of the flooded container, as seen in Figure 15b. Note that in this case, the water directly surrounds the fuel pebbles in the container, improving neutron moderation and leading to an increased fission rate compared to the case in Figure 15a where the pebbles are surrounded by air.

In all cases considered here, this system is still subcritical, and the maximum k_{eff} was found to be 0.37599 ± 0.00012, which is far below the safety limit of 0.95, suggesting that there is no criticality accident hazard under such conditions.

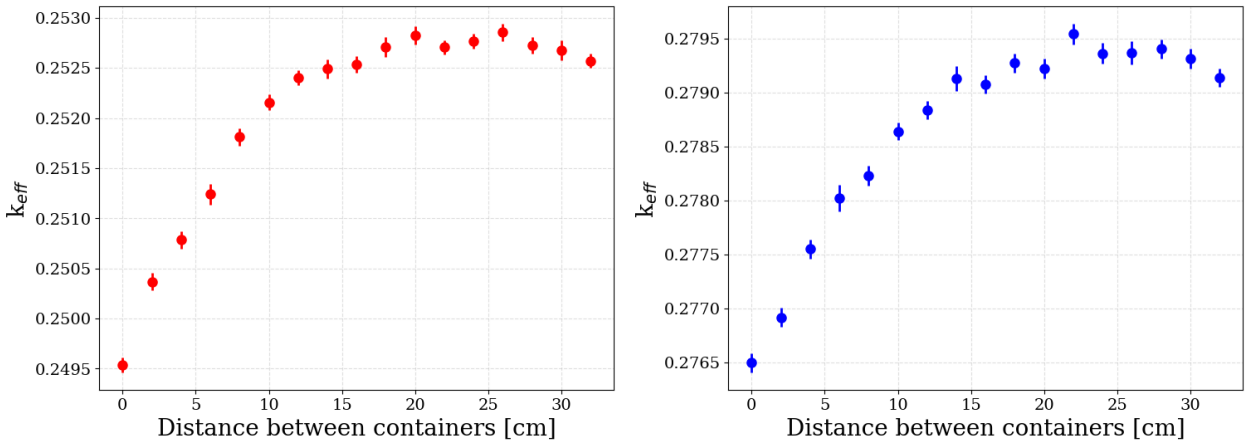

(a) packing fraction 45%

(b) packing fraction 50%

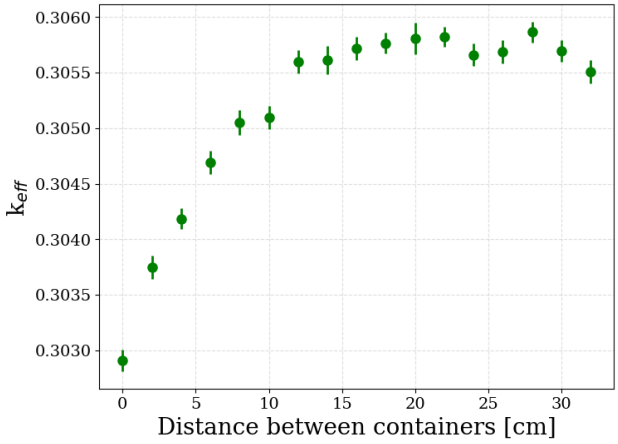

(c) packing fraction 55%

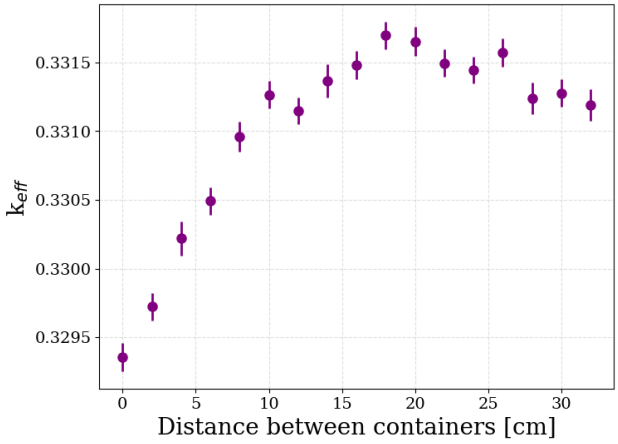

(d) packing fraction 60%

Figure 14. Change of k_{eff} with distance between the VP-55 packages. Error bars represent 1σ statistical uncertainties from the Monte Carlo calculation.

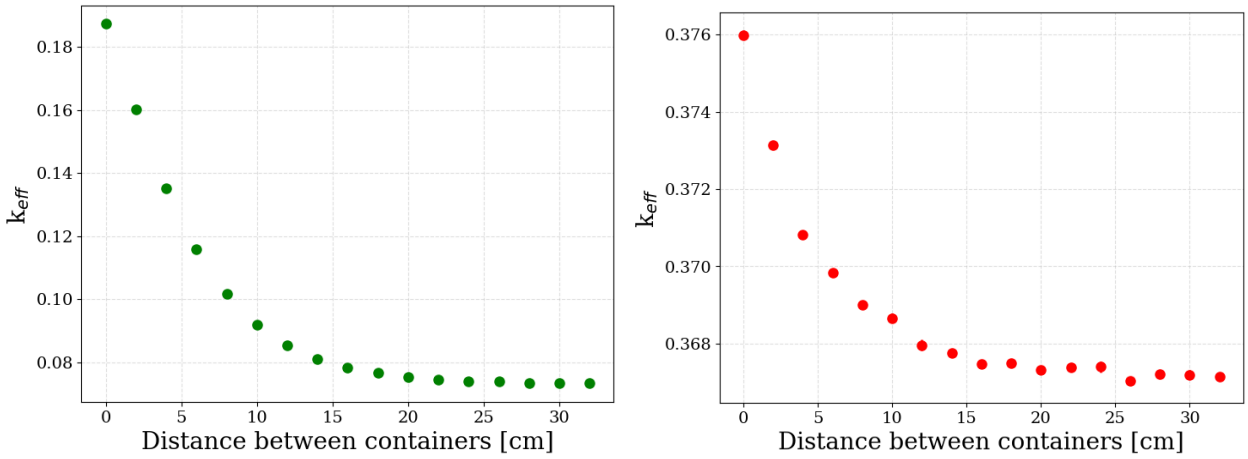

(a) Water surrounding the VP-55 package

(b) Water surrounding containers and into the container

Figure 15. Change of k_{eff} with distance between packages. Error bars represent 1σ statistical uncertainties from the Monte Carlo calculation.

5. SCENARIO 3: PEBBLE EJECTION FROM FUEL HANDLING SYSTEM

In this section, the fuel stage under consideration is the fuel handling during reactor operation. More specifically, the scenario selected here involves a rupture of the FHSS pipe, leading to pebbles' ejection from the core under elevated temperature and pressure. The PBMR-400 fuel handling system consists of a core unloading device in each of the three de-fueling chutes, from which the fuel is moved pneumatically to the burnup assaying equipment. After the burnup has been determined, the fuel is directed to the spent fuel tanks or back to the core, depending on its burnup. The fuel pebbles are re-loaded into the core through three fueling lines (Reitsma et al. 2013).

The accident under study here may occur for fuel pebbles when being directed out of the core after finishing a complete pass. Therefore, SCALE analysis involves generating an inventory of individual fuel pebbles after each pass.

5.1 SCALE METHODOLOGY FOR RAPIDLY GENERATING FUEL PEBBLE INVENTORIES

In the PBMR-400, the fuel pebbles are loaded from the top of the core and directed randomly into a flow channel or vertical trajectory. Owing to the radial and axial flux distributions in the core and the unique resident time in each pass, the incremental burnup of each fuel pebble varies with each pass, resulting in a burnup distribution of pebbles after each pass and at the time of discharge. Past research has quantified these distributions using new capabilities in SCALE/ORIGAMI developed to enhance the modeling of PBRs (Hartanto et al. 2022).

As mentioned in Section 2, one of these capabilities includes extending SCALE's ORIGAMI capability to address the depletion of flowing pebbles in PBRs (Skutnik, Bostelmann, and Wieselquist 2022). This depletion process is managed through axial (i.e., transit) zones, considering each zone's radial characteristics, such as the radial power shape, radial pebble population distribution, and radial zone library. Multiple passes of pebble depletion can be simulated, and each pass is defined by a transit history that consists of pebble power, irradiation time, cooling time, and a series of sequential transit zones that include the fractional irradiation time and the axial power factor. Using this approach, the average core-wise fuel composition can be obtained by depleting pebbles using several radial channels in a transit history. Likewise, it can be used to evaluate the burnup and inventory of a single pebble passing through different channels by depleting the pebble in a single radial channel in each transit history, as applied in this work. The procedures used are detailed in Hartanto et al. (2022), but for completeness, the basic steps are outlined below.

1. Following the PBMR-400 benchmark (Reitsma et al. 2013), the SCALE model used five radial channels for modeling the fuel regions in the core. ORIGEN libraries were generated using TRITON for each of the PBMR-400's five radial channels, employing an axial slice of the core model. This involved depleting fresh pebbles surrounded by non-depleting pebbles at their average equilibrium compositions (Skutnik and Wieselquist 2021a). The libraries cover the fuel and reflector temperatures of 700 K, 900 K, and 1200 K, and a burnup range of 0 to 100 GWd/MTU.

2. Utilizing data from Reitsma (2004) and the channel-wise flux profile, ORIGEN was used to reproduce the pebble power history required to define the transit history in each channel and pass.

3. ORIGAMI depletion calculations were conducted for a specified number of transits. Each transit history modeled a single radial flow channel with 22 transit zones. The radial channel where the pebble flows is determined randomly with a probability proportional to the channel's volume and the pebble's velocity.

4. After each pass, a cooling time of 4.5 days was assumed, and decay calculations were performed using ORIGEN.

These calculations were performed for 20,000 fuel pebbles of different operation histories, and the resulting inventory of these pebbles was stored in an inventory interface file known as `ii.json` and provided to the MELCOR team at SNL for severe accident analysis. The following section provides an analysis of the fuel inventory and decay heat of these pebbles.

5.2 ANALYSIS OF PEBBLES' INVENTORY DURING OPERATION

5.2.1 Burnup Analysis

The inventory and the burnup of the 20,000 pebbles are retrieved from the ORIGEN concentration file—f71 files—resulting from ORIGAMI calculations, and the burnup distribution after each pass is shown in Figure 16.

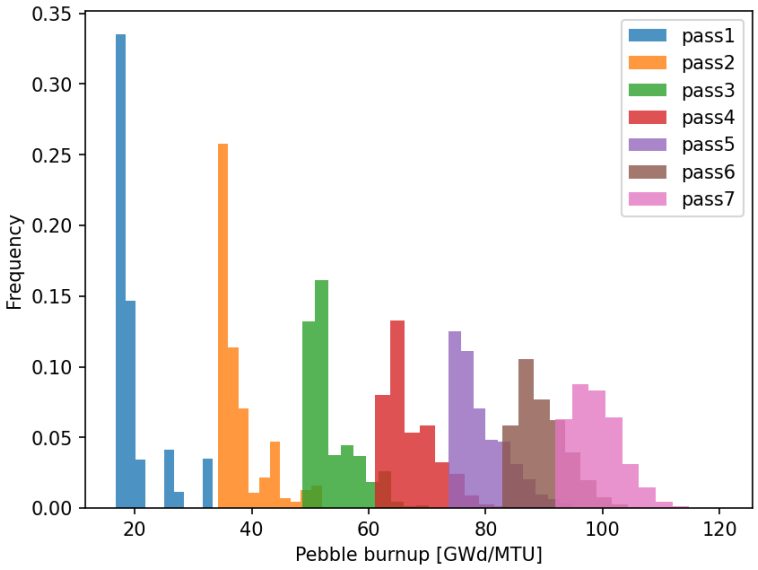

Figure 16. Relative fuel pebble burnup distribution after each pass (with the integral of data for each pass equal to 1).

Note that because the simulation allowed each pebble to complete seven passes through the core, some pebbles exceeded the target burnup of the PBMR-400 pebbles (90 GWd/MTU), as can be observed in the Figure 16. This means that some fuel pebbles that have not reached the target burnup can exceed it if sent back to the core. The after-pass burnup data are used to establish a burnup cutoff to inform decisions on whether the pebble should be returned to the core or retired and stored in the spent fuel tank. This cutoff was estimated by computing the average burnup of the retired pebbles at assumed cutoff values between 80 and 90 GWd/MTU. As shown in Figure 17, selecting a burnup limit value of 85 GWd/MTU results in an average burnup of retired pebbles close to the target value, 90 GWd/MTU.

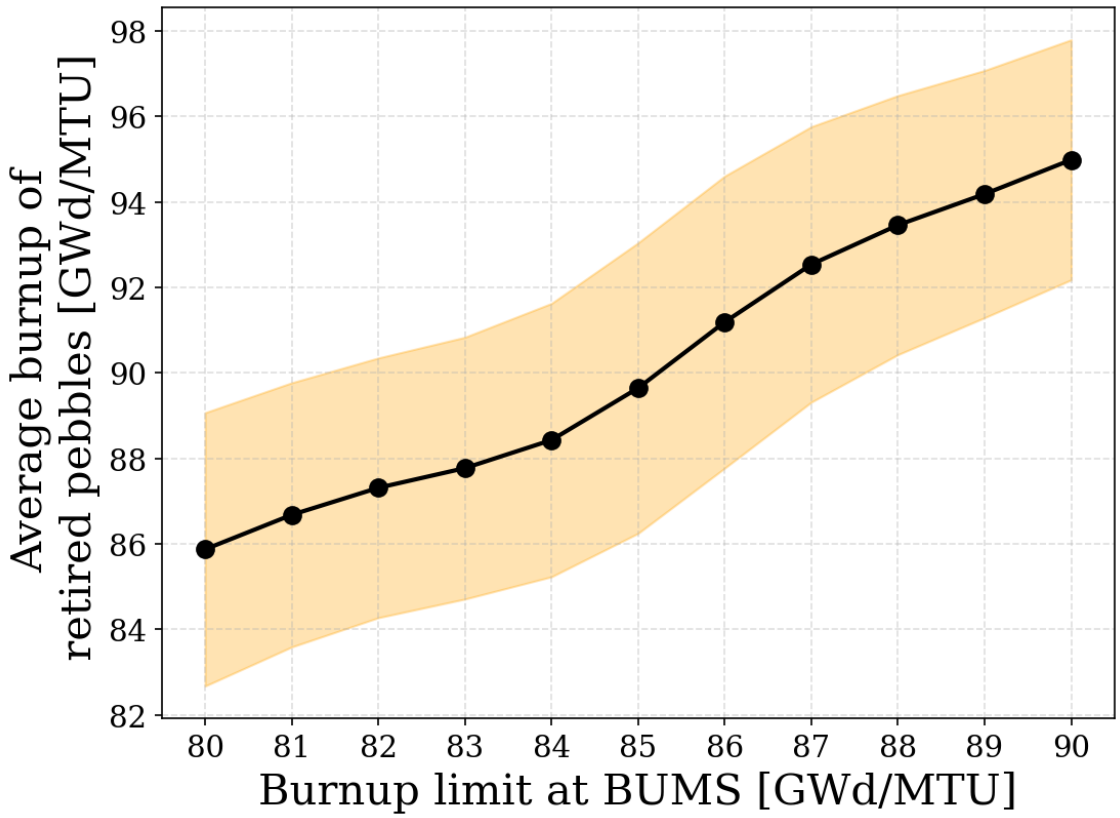

Figure 17. Average burnup of retired pebbles at different burnup limits at burnup measurement and sorting system (BUMS). The shaded area represents statistical uncertainties of 1σ resulting from the 20,000 random pebbles histories

Using this burnup cutoff value, the fractions of retired pebbles after each pass are determined and are shown in Figure 18. No pebbles are expected to be retired before pass three, whereas 80% of the pebbles are expected to complete six passes through the core before retirement.

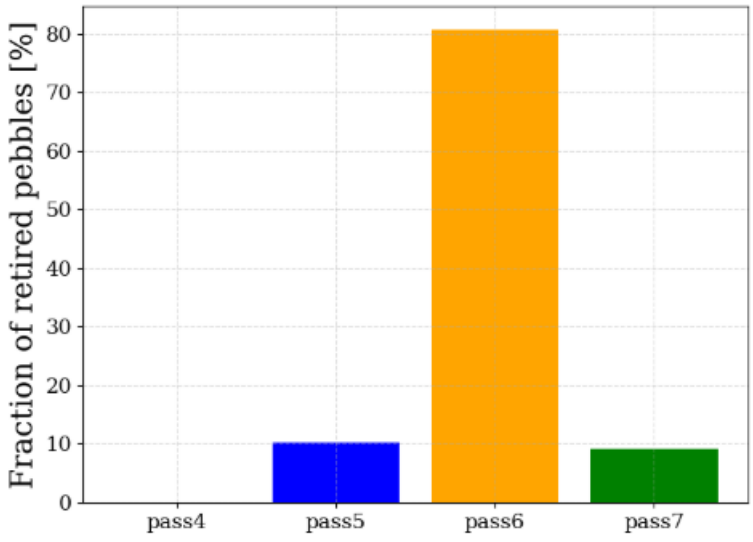

Figure 18. Fraction of retired pebbles after different passes.

5.2.2 Decay Heat Analysis

Additionally, using the generated fuel inventory, the average decay heat of a pebble after each pass was computed. Figure 19 shows the average decay heat along with the incremental burnup that the pebble undergoes in each pass. The decrease in the decay heat after each pass is due to the fuel depletion during the pass, which decreases the fission rates and, accordingly, the decay heat. Moreover, the decay time between passes allows short-lived fission products to decay.

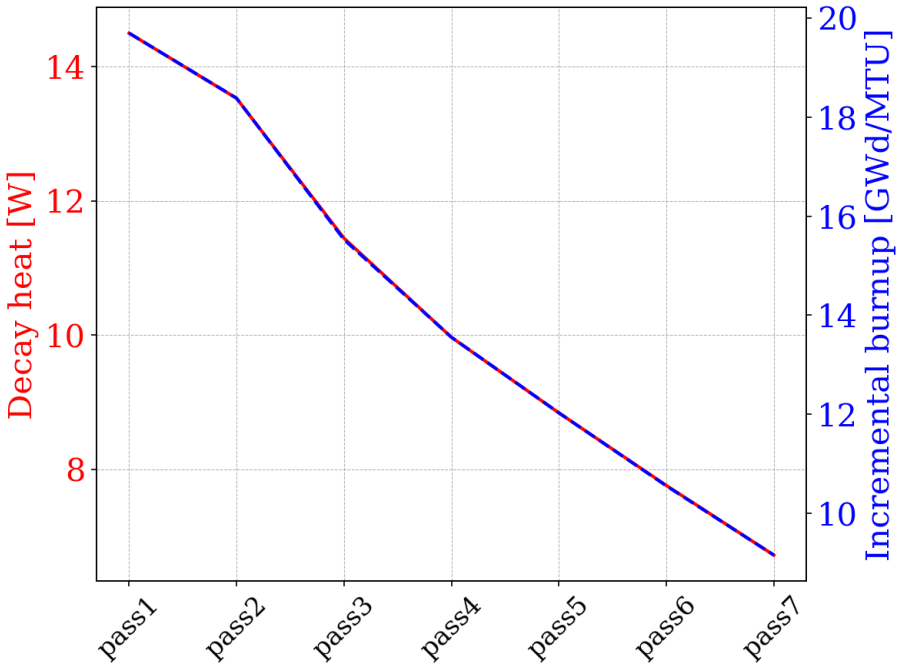

Figure 19. Average decay heat of a pebble and the incremental burnup after each pass.

To better understand this behavior, the top ten contributors to the average decay heat of a pebble after each pass were determined and are shown in Figure 20 for ten days after the end of the specific pass. One important observation is that fission products, such as ^{144}La, ^{134}I, ^{95}Nb, and others, dominate the decay heat of pebbles at early passes. After pass three, some of the actinides begin to appear in the list, such as ^{239}U and ^{239}Np, which are among the five contributors at passes five and six.

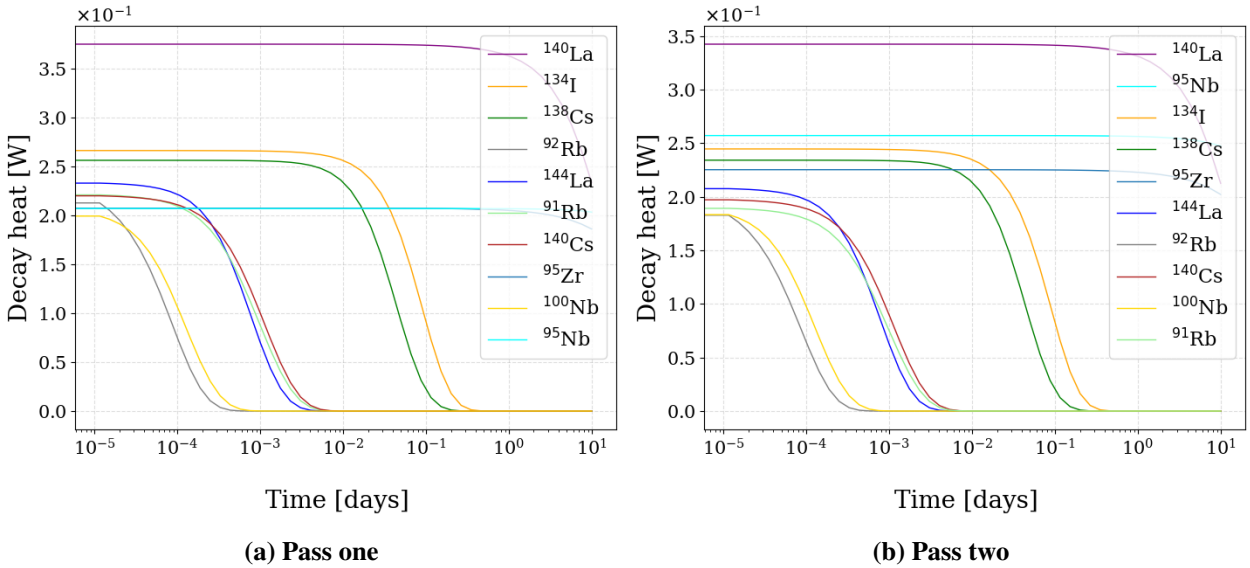

(a) Pass one

(b) Pass two

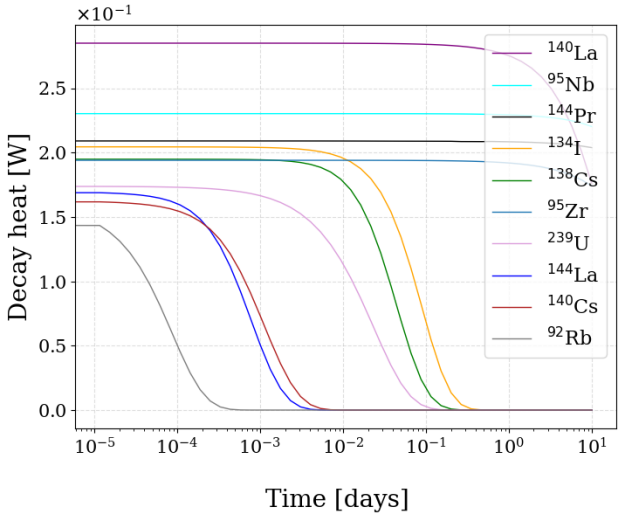

(c) Pass three

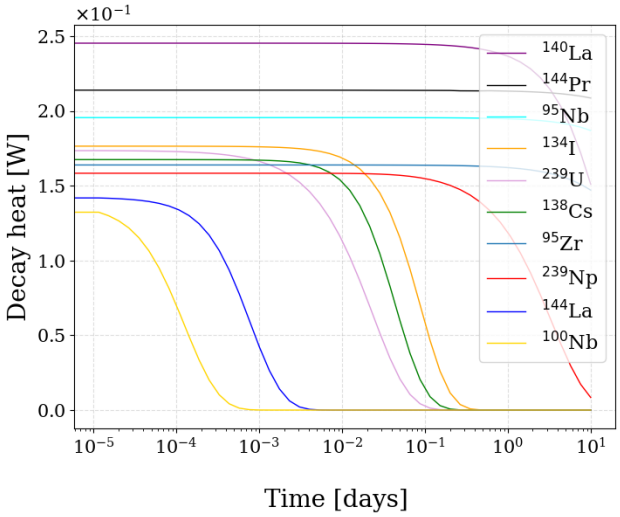

(d) Pass four

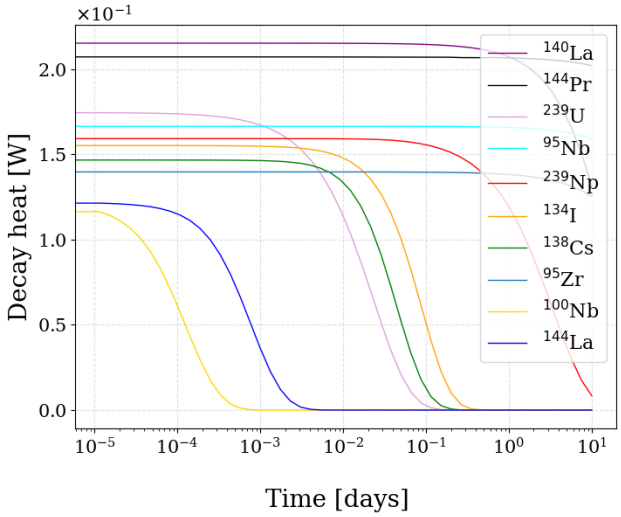

(e) Pass five

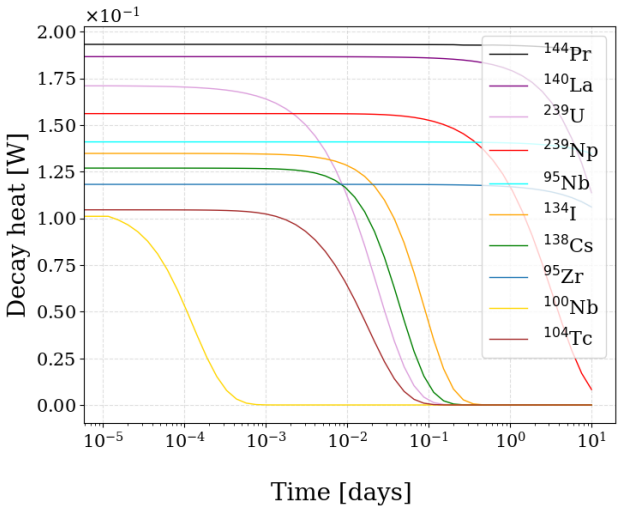

(f) Pass six

Figure 20. Top ten contributors to the decay heat after each of the six passes.

6. SCENARIO 4: COLLISION WITH THE SPENT FUEL STORAGE TANK

This section examines the scenario related to the spent fuel storage stage within the fuel cycle. The accident involves damage to the SFT that can be caused by a collision with a vehicle or suspended load. Such an incident could damage the stored spent fuel pebbles, potentially releasing fission products.

To assess the consequences of this accident, it was essential to calculate the fuel inventory of pebbles housed in the spent fuel tank. The SCALE code system was employed to compute the tank inventory based on certain assumptions, which are listed later. The resultant inventory has been shared with the MELCOR team at SNL to evaluate the accident's consequences (US NRC, ORNL, SNL 2023).

6.1 PBMR-400 SPENT FUEL TANK

Shown in Figure 21 is the FHSS of the PBMR-400, which is used for different purposes, such as moving pebbles from the core to the SFT. Ideally, more than one tank is used to store the fuel pebbles after discharge from the reactor, depending on the spent fuel tank capacity and the number of pebbles being discharged from the core during the reactor's lifetime.

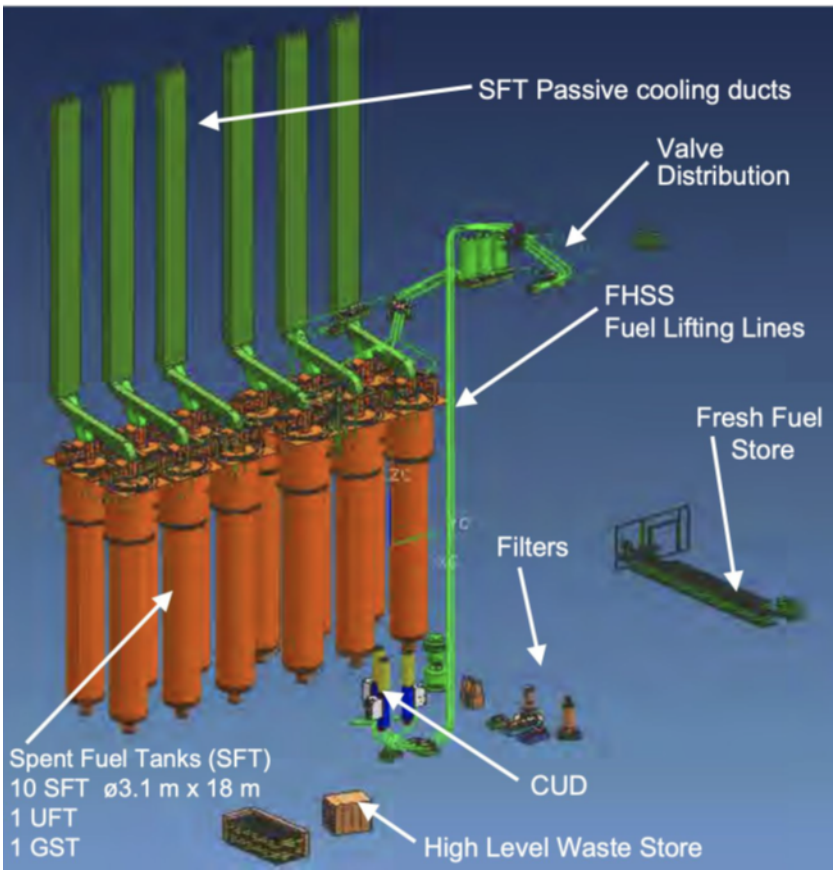

Figure 21. Spent fuel tank illustrative model (J. Slabber 2006).

6.2 SPENT FUEL TANK INVENTORY CALCULATIONS PROCEDURES

Several assumptions were incorporated to illustrate the methodology employed for establishing the inventory of the SFT, and they are listed below.

1. Following retirement, the pebbles are transported to the SFT by the FHSS.
2. Each SFT can accommodate 620,000 pebbles.
3. The discharge rate is 483 fuel pebbles per day, which implies that it takes 1,284 days to fill one tank.
4. The filling of the SFT occurs incrementally, one day at a time, resulting in a total of 1,284 layers, as depicted in Figure 22.

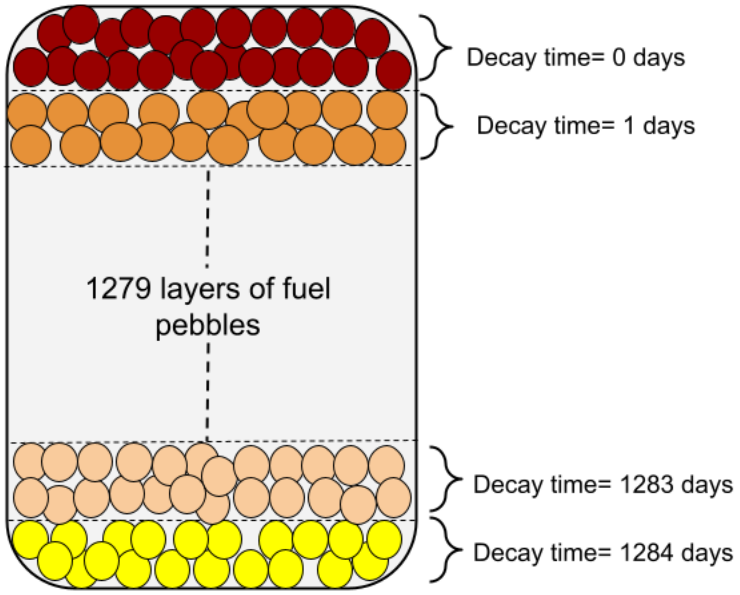

Figure 22. Illustrative figure of the SFT filling procedures.

To calculate the fuel layers inventory, the following procedures are employed:

1. Determine an average spent fuel pebble inventory after discharge from the core. This is done using the OBIWAN tool in SCALE, which blends the discharge inventory of the 20,000 pebbles utilized in the preceding scenario (see Section 5). The output of this step is an average estimate of the discharge inventory per fuel pebble.
2. Use ORIGEN to decay this average inventory over 1,284 days with a one-day time step. This yields an inventory at intervals of 1, 2, ..., 1284 decay days after discharge into the spent fuel tank. The inventory is scaled based on the number of pebbles per layer, 483. The output of this step represents the inventories of the distinct layers in the SFT.

The inventories of all layers were stored in an inventory interface file and sent to the MELCOR team at SNL to perform the accident progression analysis. The next section provides a brief analysis of the tank's decay heat.

6.3 ANALYSIS OF SPENT FUEL TANK DECAY HEAT

The total decay heat of the tank was computed by summing the individual decay heat of all layers and is shown in Figure 23 for ten days after the tank was full of discharged pebbles.

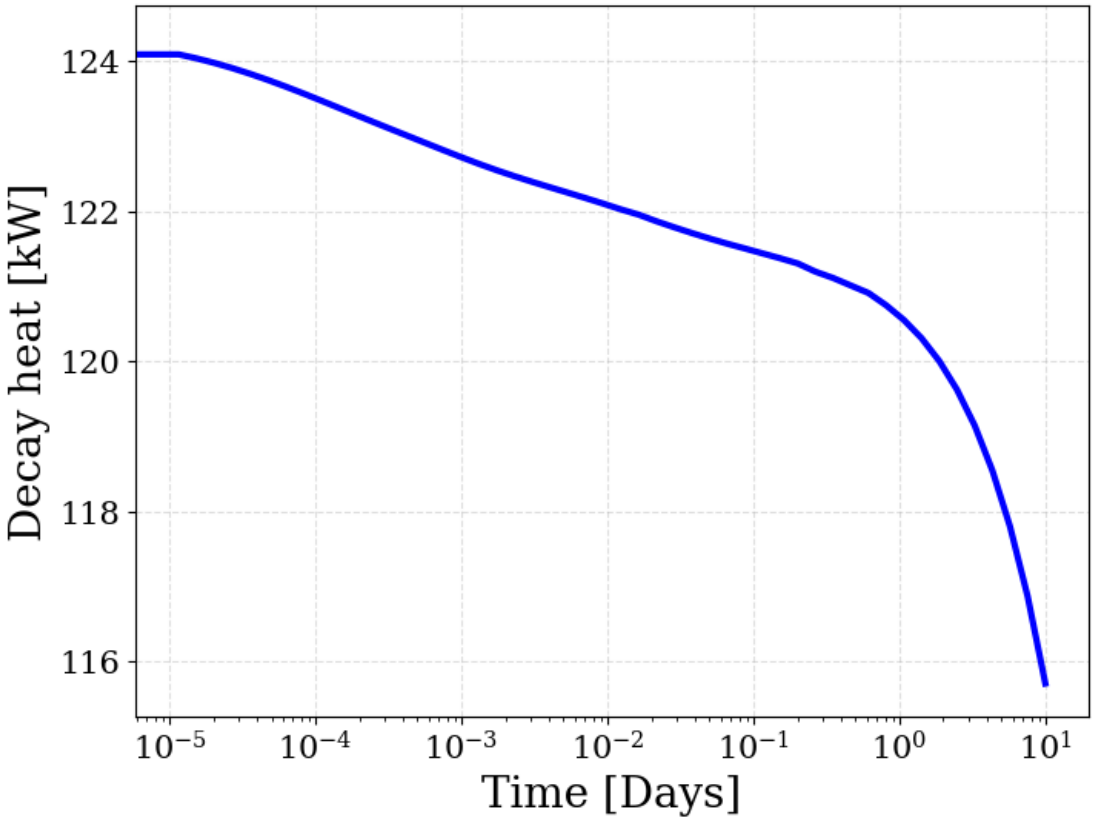

Figure 23. Total decay heat of the spent fuel tank.

As can be observed, at the time the tank is completely filled with discharged pebbles, the decay heat is approximately 124 kW, decaying slowly until it reaches about 115 kW after 10 days of discharge.

Figure 24 illustrates the change of the decay heat between different layers. As expected, the top layer of the tank has the largest contribution to the total decay heat (3%) because it contains pebbles that most recently discharged from the core; the contributions to total decay heat decrease exponentially for each successive layer down in the tank.

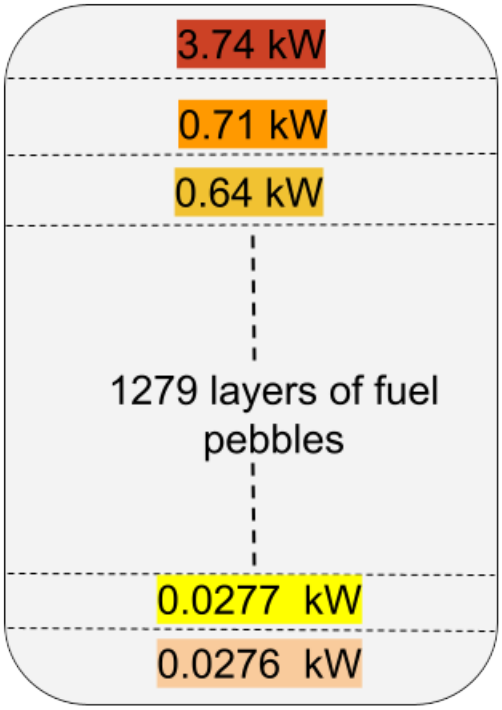

Figure 24. Illustrative figure of the decay heat values of each layer.

The top contributors to the decay heat of each layer were determined. For brevity, only those of the top, middle, and bottom layers are shown in Figure 25. The figure shows that although the top five nuclides contribute to 80–90% of the decay heat of the middle and bottom layers, they account only for 50% of the decay heat of the top layer. This is because the top layers contain the pebbles that have last discharged from the core and still contain many short-lived fission products, in addition to those daughter nuclides built up in the fuel during depletion, such as ^{144}Pr ($T_{\frac{1}{2}}$=17 min), which is an important contributor to decay heat in all layers and originates partially from ^{144}La, a direct fission product with a fission yield of approximately 1×10^{-2}. Other important nuclides contributing to the decay heat of the first layer are ^{95}Zr ($T_{\frac{1}{2}}$=64 d) and its daughter nuclide ^{95}Nb ($T_{\frac{1}{2}}$=34 d), ^{239}NP ($T_{\frac{1}{2}}$=2 d), and ^{140}La ($T_{\frac{1}{2}}$=40 s.). After a period of discharge and storage in the tank, many of the nuclides in the pebbles inventory stabilize, and the decay heat becomes dominated by fewer nuclides; thus, their relative contribution is larger, as shown in Figures 25b and 25c. For the middle and bottom layers, the same five nuclides contribute to the decay heat but with different relative contributions. These are nuclides that appear late in the decay chain, such as ^{144}Pr ($T_{\frac{1}{2}}$=17 min.), ^{106}Rh ($T_{\frac{1}{2}}$=30 sec.), ^{90}Y ($T_{\frac{1}{2}}$=64 h.), and ^{137}Ba ($T_{\frac{1}{2}}$=2 min.), or have a relatively large half-life, such as ^{134}Cs ($T_{\frac{1}{2}}$=2 y.).

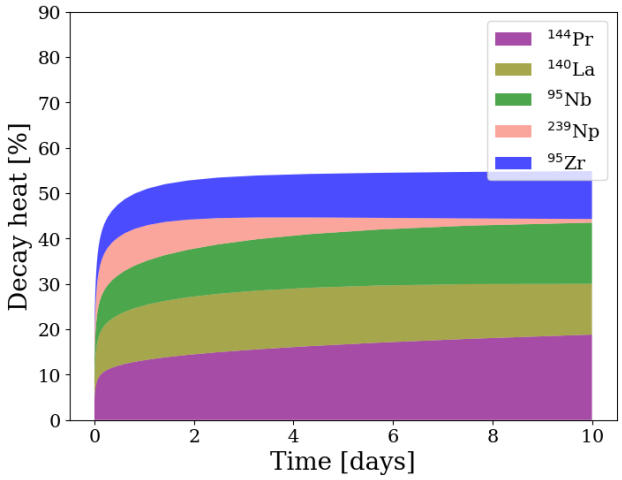

(a) Top layer
(day of discharge)

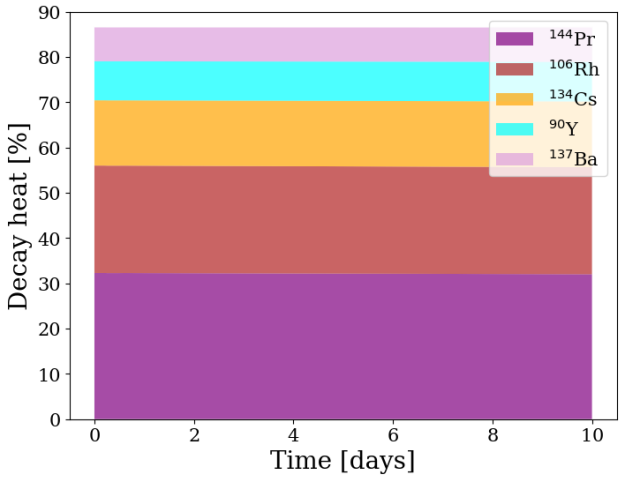

(b) Middle layer
(650 days after discharge)

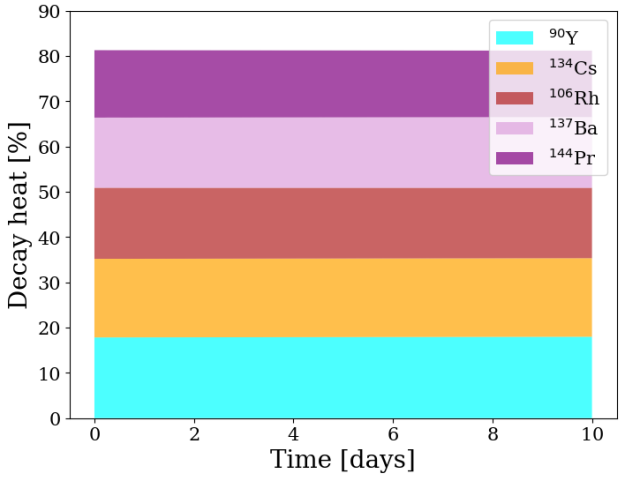

(c) Bottom layer
(1284 days after discharge)

Figure 25. Top five contributors to the decay heat of the top, middle, and bottom layers.

7. CONCLUSION

This work supports an NRC project to demonstrate the modeling and simulation of different scenarios during the fuel cycle of non-LWRs using the SCALE code system. This study focuses on the fuel cycle of the HTGR and demonstrates SCALE capabilities for HTGR criticality calculations and inventory generation. Four accident scenarios in four distinct stages of the HTGR fuel cycle were selected as demonstrative examples of the use of SCALE to simulate accident scenarios in the HTGR fuel cycle, motivating other work to simulate different scenarios, whether within the same stages addressed here or other stages not addressed. The scenarios were selected to span different stages and to show different SCALE analyses. The PBMR-400 was selected as the reference design in all calculations.

The first scenario demonstrated SCALE criticality calculations for scenarios of water ingress into the two variants of the recently certified DN30-X package transporting UF_6 at HALEU enrichment levels: DN30-10 for 10 wt% and DN30-20 for 20 wt% enrichment. In addition to modeling different water ingress scenarios, the impact of package spacing was studied for an infinite lattice of DN30-X packages. From all considered calculations, the highest k_{eff} was found to be 0.64266 ± 0.00011 for the case of the DN30-20 package with water between containers. The k_{eff} value being significantly below critical implies no criticality accident hazard under the simulated conditions.

The second scenario demonstrated SCALE criticality calculations for scenarios of fresh pebbles' transportation in the Versa-Pac 55 transportation package. Scenarios of container damage or a drop in which package spacing was reduced were considered, as well as different water ingress scenarios. SCALE's capabilities for fast MG calculations of double-heterogeneous fuel systems as well as recent enhancements for explicit TRISO fuel particle modeling in CE calculations were highlighted. The most limiting case was the flooding scenario while the containers are touching. The maximum k_{eff} was found to be 0.37599 ± 0.00012 for an infinite lattice of packages in which water is flooding the packages. This maximum k_{eff} is still significantly subcritical and far below the criticality safe limit of 0.95, implying that no criticality accident is expected under the simulated conditions.

The third scenario demonstrated HTGR inventory generation with SCALE to support MELCOR accident progression calculations of a scenario during reactor operation in which a pipe rupture results in pebbles moving out of the core. Thanks to recent capability extensions in SCALE's ORIGAMI tool to treat flowing fuel in PBRs, inventories for 20,000 pebbles were rapidly generated to compute a representative average inventory per pebble after they completed each pass through the core.

The fourth and final scenario in this study demonstrated HTGR inventory generation and decay heat analysis to support an accident scenario from the damage of a fully loaded SFT in which fuel pebbles are stored after their discharge. Based on assumptions regarding the tank capacity and the rate of pebbles discharged daily, the inventory was generated using information about 20,000 pebbles, the inventory for which was generated in the third scenario. The decay heat was studied, and it was found that a SFT that was just fully filled with a total of 620,000 fuel pebbles has a total decay heat of 124 kW, with 3% of the decay heat being produced by less than 0.1% of the fuel pebbles at the very top of the tank, since these were recently discharged. The inventory was post-processed and transferred to the MELCOR team to proceed with the accident progression (US NRC, ORNL, SNL 2023).

8. REFERENCES

Bostelmann, F., C. Celik, R. F. Kile, and W. A. Wieselquist. 2022. *SCALE Analysis of a Fluoride Salt-Cooled High-Temperature Reactor in Support of Severe Accident Analysis.* Technical report ORNL/TM-2021/2273. Oak Ridge, TN: Oak Ridge National Laboratory. https://doi.org/10.2172/1854475.

Bostelmann, F., C. Celik, M. L. Williams, R. J. Ellis, G. Ilas, and W. A. Wieselquist. 2020. "SCALE capabilities for high temperature gas-cooled reactor analysis." *Annals of Nuclear Energy* 147:107673. https://doi.org/10.1016/j.anucene.2020.107673.

Bostelmann, F., E. E. Davidson, W. A. Wieselquist, D. Luxat, K. C. Wagner, and L. I. Albright. 2023. *Non-LWR Fuel Cycle Scenarios for SCALE and MELCOR Modeling Capability Demonstration.* Technical report ORNL/TM-2023/2954. Oak Ridge, TN: Oak Ridge National Laboratory. https://doi.org/10.2172/2251628.

Brown, D.A., M.B. Chadwick, R. Capote, A.C. Kahler, A. Trkov, M.W. Herman, A.A. Sonzogni, et al. 2018. "ENDF/B-VIII.0: The 8th Major Release of the Nuclear Reaction Data Library with CIELO-project Cross Sections, New Standards and Thermal Scattering Data." *Nuclear Data Sheets* 148:1–142. https://doi.org/10.1016/j.nds.2018.02.001.

Chadwick, M.B., M. Herman, P. Obložinský, M.E. Dunn, Y. Danon, A.C. Kahler, D.L. Smith, et al. 2011. "ENDF/B-VII.1 Nuclear Data for Science and Technology: Cross Sections, Covariances, Fission Product Yields and Decay Data." *Nuclear Data Sheets* 112 (12): 2887–2996. https://doi.org/10.1016/j.nds.2011.11.002.

DAHER. 2019. *Safety Analysis Report DN30 Package.* DAHER. https://www.nrc.gov/docs/ML1920/ML19200A133.pdf.

DAHER-TLI. 2018. *Versa-Pac Safety Analysis Report.* DAHER-TLI. https://www.nrc.gov/docs/ML1833/ML18330A093.pdf.

De Hart, M. D., and Stephen M. Bowman. 2011. "Reactor Physics Methods and Analysis Capabilities in SCALE." *Nuclear Technology* 174 (2): 196–213. https://doi.org/10.13182/NT174-196.

Detwiler, Rebecca S, Ronald J McConn, Thomas F Grimes, Scott A Upton, and Eric J Engel. 2021. *Compendium of material composition data for radiation transport modeling.* Technical report. Pacific Northwest National Lab.(PNNL), Richland, WA (United States). https://www.pnnl.gov/main/publications/external/technical_reports/PNNL-15870Rev2.pdf.

Gauld, I. C., G. Radulescu, G. Ilas, B. D. Murphy, M. L. Williams, and Dorothea Wiarda. 2011. "Isotopic Depletion and Decay Methods and Analysis Capabilities in SCALE." *Nuclear Technology* 174 (2): 169–195. https://doi.org/10.13182/NT11-3.

Ghaddar, Tarek, Friederike Bostelmann, Tara Pandya, and Matthew Jessee. 2024. "Modeling Enhancements and Benchmarking of Pebble Bed Reactors in the Shift Monte Carlo Code." In *International Conference on Physics of Reactors 2024 (PHYSOR 2024), San Francisco, CA, April 21–24.*

Goluoglu, Sedat, Lester M Petrie Jr, Michael E Dunn, Daniel F Hollenbach, and Bradley T Rearden. 2011. "Monte Carlo criticality methods and analysis capabilities in SCALE." *Nuclear Technology* 174 (2): 214–235. https://doi.org/10.13182/NT10-124.

Hartanto, Donny, William Wieselquist, Steve Skutnik, Philip Gibbs, and Donald N Kovacic. 2022. "Uncertainty Quantification of Pebble's Discharge Burnup and Isotopic Inventory using SCALE." In *Trans. Am. Nucl. Soc. 127,* 1040–1043. November. https://www.osti.gov/servlets/purl/1905409.

Humphries, L. L., B. A. Beeny, F. Gelbard, D. L. Louie, J. Phillips, R. C. Schmidt, and N. E. Bixler. 2021. *MELCOR Computer Code Manuals - Vol. 1: Primer and Users' Guide Version 2.2.18019.* Technical report SAND2021-0726 O. Albuquerque, NM: Sandia National Laboratories. https://www.nrc.gov/docs/ML2104/ML21042B319.pdf.

J. Slabber. 2006. *Reactor Unit and Main Support Systems.* https://www.nrc.gov/docs/ML0606/ML060680079.pdf.

Kim, Kang Seog, Andrew M Holcomb, Rike Bostelmann, Dorothea Wiarda, Brandon R Langley, and William Wieselquist. 2021. "Improvement of the SCALE-XSProc Capability for High-Temperature Gas-Cooled Reactor Analysis." In *International Conference on Mathematics and Computational Methods Applied to Nuclear Science and Engineering (M&C 2021).* Oak Ridge National Lab.(ORNL), Oak Ridge, TN (United States). https://www.osti.gov/biblio/1826043.

Lo, A., F. Bostelmann, D. Hartanto, B. Betzler, and W. A. Wieselquist. 2022. *Application of SCALE to Molten Salt Fueled Reactor Physics in Support of Severe Accident Analyses.* Technical report ORNL/TM-2022/1844. Oak Ridge, TN: Oak Ridge National Laboratory. https://doi.org/10.2172/1897864. https://www.osti.gov/biblio/1897864.

Orano, Hanau. 2022. *Safety Analysis Report for the DN30-X Package.* Orano, Germany. https://www.nrc.gov/docs/ML2232/ML22327A183.pdf.

Pandya, T., T. Ghaddar, F. Bostelmann, M. Jessee, and P. Britt. 2023. *Modeling Enhancements and Demonstration of Shift Capabilities for PBRs and MSRs.* Technical report ORNL/TM-2023/3072. Oak Ridge, TN: Oak Ridge National Laboratory. https://www.osti.gov/biblio/2203030.

Pandya, T. M., S. R. Johnson, T. M. Evans, G. G. Davidson, S. P. Hamilton, and A. T. Godfrey. 2016. "Implementation, Capabilities, and Benchmarking of Shift, a Massively Parallel Monte Carlo Radiation Transport Code." *Journal of Computational Physics* 308:239–272. https://doi.org/10.1016/j.jcp.2015.12.037.

Reitsma, Frederik. 2004. "The pebble bed modular reactor layout and neutronics design of the equilibrium cycle." In *International Conference on Physics of Reactors 2004 (PHYSOR 2004), Chicago, Illinois, April 25-29.* https://www.ipen.br/biblioteca/cd/physor/2004/PHYSOR04/papers/96100.pdf.

Reitsma, Frederik, Kostadin Ivanov, Enrico Sartori, Hyun Chul Lee, Antti Daavittila, Jaakko Leppanen, Enrico Girardi, Maurice Grimod, Oliver Koeberl, Simone Massara, et al. 2013. *PBMR Coupled Neutronics/Thermal-hydraulics Transient Benchmark. The PBMR-400 Core Design-Volume 1 The Benchmark Definition.* Technical report. Organisation for Economic Co-Operation and Development.

Shaw, A., F. Bostelmann, D. Hartanto, E. Walker, and W. A. Wieselquist. 2023. *SCALE Modeling of the Sodium-Cooled Fast-Spectrum Advanced Burner Test Reactor.* Technical report ORNL/TM-2022/2758. Oak Ridge, TN: Oak Ridge National Laboratory. https://doi.org/10.2172/1991734.

Skutnik, S. E., and W. A. Wieselquist. 2021a. *Assessment of ORIGEN Reactor Library Development for Pebble-Bed Reactors Based on the PBMR-400 Benchmark.* Technical report ORNL/TM-2020/1886. Oak Ridge, TN: Oak Ridge National Laboratory. https://doi.org/10.2172/1807271.

Skutnik, S. E., and W. A. Wieselquist. 2021b. *Assessment of ORIGEN Reactor Library Development for Pebble-Bed Reactors Based on the PBMR-400 Benchmark.* Technical report ORNL/TM-2020/1886. Oak Ridge, TN: Oak Ridge National Laboratory. https://doi.org/10.2172/1807271.

Skutnik, S.E., F. Bostelmann, and W.A. Wieselquist. 2022. "Rapid Depletion Analysis of Flowing-Pebble Reactor Systems at Equilibrium using SCALE." In *International Conference on Physics of Reactors 2022 (PHYSOR 2022),* 1298–1307. May. https://doi.org/10.13182/PHYSOR22-37367.

US NRC. 2019. *CERTIFICATE OF COMPLIANCE No.9362.* US Nuclear Regulatory Commission. https://www.nrc.gov/docs/ML2307/ML23073A056.pdf.

US NRC. 2020. *NRC Non-Light Water Reactor (Non-LWR) Vision and Strategy, Volume 3: Computer Code Development Plans for Severe Accident Progression, Source Term, and Consequence Analysis.* Technical report ML20030A178, Rev. 1. Rockville, MD: US Nuclear Regulatory Commission. https://www.nrc.gov/docs/ML2003/ML20030A178.pdf.

US NRC. 2021. *NRC Non-Light Water Reactor (Non-LWR) Vision and Strategy, Volume 5: Radionuclide Characterization, Criticality, Shielding, and Transport in the Nuclear Fuel Cycle.* Technical report ML21088A047, Rev. 1. Rockville, MD: US Nuclear Regulatory Commission. https://www.nrc.gov/docs/ML2108/ML21088A047.pdf.

US NRC. 2022. *CERTIFICATE OF COMPLIANCE No.9342.* US Nuclear Regulatory Commission. https://www.nrc.gov/docs/ML1025/ML102510693.pdf.

US NRC. 2023. *CERTIFICATE OF COMPLIANCE No.9388.* US Nuclear Regulatory Commission. https://www.nrc.gov/docs/ML2308/ML23083B978.pdf.

US NRC, ORNL, SNL. 2023. *SCALE & MELCOR non-LWR Fuel Cycle Demonstration Project - High Temperature Gas-Cooled Reactors.* https://www.nrc.gov/docs/ML2305/ML23058A213.pdf. Accessed: November 6, 2023.

Walker, E., S. E. Skutnik, W. A. Wieselquist, A. Shaw, and F. Bostelmann. 2021. *SCALE Modeling of the Fast-Spectrum Heat Pipe Reactor.* Technical report ORNL/TM-2021/2021. Oak Ridge, TN: Oak Ridge National Laboratory. https://doi.org/10.2172/1871124.

Wieselquist, W., and R. A. Lefebvre. 2023. *SCALE 6.3.1 User Manual.* Technical report ORNL/TM-SCALE-6.3.1. Oak Ridge, TN: Oak Ridge National Laboratory. https://doi.org/10.2172/1959594.